Bunburra Rockhole: Exploring the geology of a new differentiated asteroid

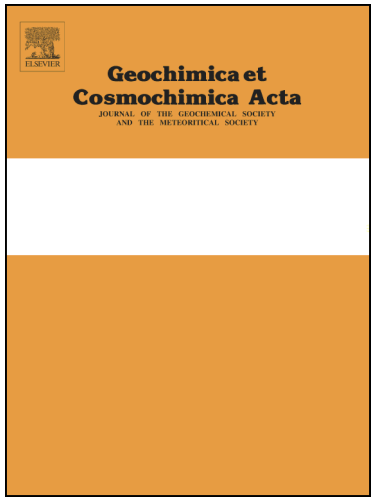

Bunburra Rockhole: Exploring the Geology of a new differentiated asteroid

G.K. Benedix, P.A. Bland, J.M. Friedrich, D.W. Mittlefehldt, M.E. Sanborn, Q.-Z. Yin, R.C. Greenwood, I.A. Franchi, A.W.R. Bevan, M.C. Towner, G.C. Perotta, S.A. Mertzman

PII: S0016-7037(17)30191-6
DOI: http://dx.doi.org/10.1016/j.gca.2017.03.030
Reference: GCA 10212

To appear in: *Geochimica et Cosmochimica Acta*

Received Date: 17 August 2016
Revised Date: 25 February 2017
Accepted Date: 21 March 2017

Please cite this article as: Benedix, G.K., Bland, P.A., Friedrich, J.M., Mittlefehldt, D.W., Sanborn, M.E., Yin, Q.-Z., Greenwood, R.C., Franchi, I.A., Bevan, A.W.R., Towner, M.C., Perotta, G.C., Mertzman, S.A., Bunburra Rockhole: Exploring the Geology of a new differentiated asteroid, *Geochimica et Cosmochimica Acta* (2017), doi: http://dx.doi.org/10.1016/j.gca.2017.03.030

Bunburra Rockhole: Exploring the Geology of a new differentiated asteroid.

G.K. Benedix[1,2], P. A. Bland[1,2], J.M. Friedrich[3,4], D.W. Mittlefehldt[5], M.E. Sanborn[6], Q.-Z. Yin[6], R.C. Greenwood[7], I.A. Franchi[7], A.W.R. Bevan[2], M.C. Towner[1], G.C. Perotta[4] and S.A. Mertzman[8]

[1] Curtin University, Applied Geology, Bentley, Western Australia, Australia

[2] Western Australia Museum, Department of Earth and Planetary Sciences, Welshpool, Western Australia, Australia

[3] American Museum of Natural History, Earth and Planetary Sciences New York, New York, United States

[4] Fordham University, Chemistry New York, New York, United States

[5] NASA/Johnson Space Center, Houston, Texas, United States

[6] University of California, Davis, Earth and Planetary Sciences, Davis, California, United States

[7] The Open University, Planetary and Space Sciences, Milton Keynes, United Kingdom

[8] Franklin and Marshall College, Earth and Environment Lancaster, Pennsylvania, United States

Abstract

Bunburra Rockhole is the first recovered meteorite of the Desert Fireball Network. We expanded a bulk chemical study of the Bunburra Rockhole meteorite to include major, minor and trace element analyses, as well as oxygen and chromium isotopes, in several different pieces of the meteorite. This was to determine the extent of chemical heterogeneity and constrain the origin of the meteorite. Minor and trace element analyses in all pieces are exactly on the basaltic eucrite trend. Major element analyses show a slight deviation from basaltic eucrite compositions, but not in any systematic pattern. New oxygen isotope analyses on 23 pieces of Bunburra Rockhole shows large variation in both $\delta^{17}O$ and $\delta^{18}O$, and both are well outside the HED parent body fractionation line. We present the first Cr isotope results of this rock, which are also distinct from a majority of HEDs. Detailed computed tomographic scanning and back-scattered electron mapping do not indicate the presence of any other meteoritic contaminant (contamination is also unlikely based on trace element chemistry). We therefore conclude that Bunburra Rockhole represents a sample of a new differentiated asteroid, one that may have more variable oxygen isotopic compositions than 4 Vesta. The fact that Bunburra Rockhole chemistry falls on the eucrite trend perhaps suggests that multiple objects with basaltic crusts accreted in a similar region of the Solar System.

1. Introduction

Meteorites allow us to study the geology of planetary bodies other than Earth, giving insight into the processes that affect not only Earth, but all rocky planets and planetesimals in the Solar System. Depending on source material, these rocks reveal information about the initial composition of the Solar System as well as how geologic processes, such as differentiation or impact, affect that composition. Meteorites that sample differentiated bodies are called achondrites and the vast majority of this class is basaltic in composition. In this study, we present new chemical and petrologic results on a basaltic achondrite, Bunburra Rockhole, and discuss it's relationship to other achondritic meteorites. The largest group of achondrites (with 1720 members according to the Meteoritical Bulletin, accessed on 02/05/16) is the howardite, eucrite, and diogenite (HED) group, with the basaltic member (eucrites) making up over half of the group (982). HEDs are thought to come from 4 Vesta based on the match between the spectral reflectance characteristics of the meteorites and asteroid (McCord et al., 1970; Binzel and Xu, 1993). Recent results from the Dawn mission support this (McSween et al., 2013). The uniform oxygen isotopic compositions with respect to $\Delta^{17}O$ for nearly all of the meteorites in this group is considered evidence that they are from the same parent body.

Oxygen isotopes provide a means of assessing the original source of individual achondritic meteorite samples (Clayton, 1999; Clayton and Mayeda, 1984, 1996; Franchi, 2008). This is because, although their $\delta^{17}O$ and $\delta^{18}O$ values will vary as a result of mass-dependent fractionation processes, defining lines with a slope of approximately 0.52, their $\Delta^{17}O$ ($\Delta^{17}O = \delta^{17}O - \sim 0.52\ \delta^{18}O$) compositions will be specific to their source asteroid (Franchi, 2008). While the original materials from which a differentiated asteroid accreted would certainly have had widely varying $\Delta^{17}O$ compositions (Yurimoto et al., 2007), such early-formed bodies are likely to have undergone large-scale melting in response to the decay of short-lived radiogenic isotopes, such as ^{26}Al (e.g. Hevey and Sanders, 2006), thus leading to near-total isotopic homogenization (Greenwood et al., 2014). Thus, $\Delta^{17}O$, which is essentially a measure of the deviation of a suite of samples from the terrestrial fractionation line, provides an important means of assessing the provenance of meteoritical samples. Indeed, the Martian meteorites are grouped together based on their oxygen isotopic composition, as the definitive atmospheric evidence for Martian origin exists in only a few samples (Clayton and Mayeda, 1996; Pepin, 1985). However, recent works have shown that using $\Delta^{17}O$ alone as an indicator as a genetic link for planetary materials can be ambiguous (e.g. Sanborn et al., 2014).

Based on existing achondrite meteorite compositions, differentiation processes, do not commonly affect the bodies that deliver meteorites to the Earth. Of the ~55,000 officially named meteorites in collections, about 3500 (6%) probably come from bodies that experienced the full separation into core, mantle and crust . Of those, 1745 (~50%) likely sample the crust and, possibly, mantle of a single body, 4 Vesta (http://www.lpi.usra.edu/meteor/metbull.php). Similarly, based on physical and spectral properties, differentiated asteroids do not appear to be common in the main belt (Gradie and Tedesco, 1982; Grimm and McSween, 1993; Burbine et al., 2002), indicating that this was a rare process in the early Solar System. This is, however, contradicted by the fact that iron meteorites may sample the cores of up to 60 asteroidal bodies (Scott, 1979; Wasson, 1990). One model proposed to explain the apparent lack of differentiated asteroids in the main belt, suggests that this process occurred early, in the terrestrial planet region. Objects forming here experienced accelerated collisional evolution (in many cases removing mantles), with the survivors finding stable orbits in the main belt following close interactions with planetary embryos (Bottke et al., 2006).

The total number of meteorites that represent crustal material is ~1100, with 980 belonging to one group (eucrites) although oxygen isotopic compositions have not been measured for all 980 samples; the remaining meteorites belong to two groups – angrites with 24 members and aubrites with 72 members (these numbers include paired stones) - with vastly different mineral chemistry as well as oxygen isotopic composition. Angrites, while being broadly basaltic in composition, are

composed of augite with essentially pure anorthite, olivine and troilite, are critically understaturated with respect to SiO_2 content and have distinct oxygen isotopic compositions (Mittlefehldt et al., 1998; Greenwood et al., 2005; Keil, 2012). The aubrites are highly reduced pyroxenites that likely represent the melted surface of an enstatite-rich starting composition (Keil, 2010). Thus, our understanding of differentiation in the early solar system is hampered by having only a few bodies to examine. The identification of meteorites that are potentially from new differentiated bodies is vital to widening our knowledge of this process in the early solar system.

A number of basaltic meteorites have recently been shown to have oxygen compositions that lie significantly away from the HED mass fractionation line ($\Delta^{17}O = -0.246 \pm 0.016‰$). (Yamaguchi et al., 2002; Friedrich et al., 2003; Greenwood et al., 2005; 2014; Lentz et al., 2007; Scott et al., 2009; Wolf et al., 2009). Although having similar texture and chemistry to eucrites, some differences exist in minor element ratios. This has led some researchers to suggest that some fraction of these rocks are not from 4 Vesta (Mittlefehldt, 2005; Scott et al., 2009; Sanborn and Yin, 2014; 2016; Sanborn et al., 2016) an observation that has significance for the diversity of differentiated objects in the early Solar System.

Recent recognition that some of these rocks are 'contaminated' with minor amounts of chondritic material (Janots et al., 2012) has called into doubt this simple interpretation of oxygen isotope anomalies equating to non-HED parent body. Contamination by at least 20% H chondrite and mixing due to impact (Janots et al., 2012) is what accounts for the anomalous oxygen isotope signature found in the highly shocked howardite Jiddat al Harasis (JaH) 556. Thus, there are now a number of possibilities that might explain differences in oxygen isotopic composition. It may not be as simple as a different parent body. Note, however, that some of the O-anomalous rocks are unbrecciated or monomict eucrites and chondritic contamination thus seems unlikely (Mittlefehldt, 2005; Mittlefehldt et al., 2016).

Another explanation for anomalous oxygen isotopes might be as a result of a heterogeneous parent body. Greenwood et al. (2005) proposed that the narrow values of oxygen isotopes found in the HED and angrite meteorites indicate they were formed on separate bodies that experienced homogenization by global melting (>50%) processes. However, Wiechert et al. (2004) suggested that the magma ocean on 4 Vesta may not have fully equilibrated the oxygen isotopic composition of the planetesimal. Thus, meteorites with similar mineralogy, chemistry and texture, but different oxygen isotopic composition could sample different areas of 4 Vesta. No physical mechanism was proposed that would enable a large differentiated object, with a complex and extended geological history post-formation, to remain unequilibrated with respect to oxygen. If it were possible, it would

have far-reaching implications for our understanding of planetary differentiation, and the evolution of planetesimals in the early Solar System.

In this study, the focus is on Bunburra Rockhole (Bland et al., 2009) as a case study to probe the various hypotheses that have sought to explain anomalous basaltic achondrites. Bunburra Rockhole was the first meteorite recovered by the Desert Fireball Network - a network of cameras based in the Australian outback, designed to track fireballs and recover the associated meteorites (Bland et al., 2012) in order to link orbital and compositional data. Bunburra Rockhole was initially classified as a basaltic eucrite, based on texture, mineralogy, and mineral chemistry (Weisberg et al., 2009). Additionally, a cosmic ray exposure age of 22 Myr (Welten et al., 2012) made it the first anomalous basaltic achondrite to overlap one of the main age peaks of the HEDs. However, Bunburra Rockhole had an unusual Aten-type orbit prior to entering the Earth's atmosphere (Spurný et al., 2012). Similarly, initial oxygen isotopic analyses showed an anomalous composition ($\Delta^{17}O$ = -0.112±0.042‰; (Bland et al., 2009)), shifted from the HED fractionation line, raising questions about a link to the HED parent body.

Bunburra Rockhole is similar in many respects to basaltic eucrites. Mineral major (Fe/Mn, Fe/Mg, Fs, Wo, and An) and trace element (Ti, Zr, Y) compositions (Spivak-Birndorf et al., 2015) overlap completely the ranges of those elements in basaltic eucrites (Mittlefehldt, 2015). Furthermore, the bulk trace element composition of Bunburra Rockhole is identical to basaltic eucrites when compared to chondrite-normalized values. The bulk rare earth element pattern is generally flat, or very slightly Eu depleted, at 10× CI on average and coincides with the range of values for basaltic eucrites. The Pb-Pb and Al-Mg chronology of Bunburra Rockhole is similarly indistinguishable from the basaltic eucrites (Spivak-Birndorf et al., 2015).

Given the orbital data and anomalous oxygen isotopic composition, Bunburra Rockhole presents an excellent opportunity to explore how it might be related to other basaltic achondrites and to evaluate the implications of it's petrogenesis. Thus, we set out to confirm the nature and source of Bunburra Rockhole by undertaking a correlated study of the bulk chemical and stable isotopes of several lithologic fragments. Our goals are to establish whether those differences are best explained by contamination, an isotopically unequilibrated HED parent asteroid or a differentiated parent body distinct from 4 Vesta, and explore the implications for understanding the formation of differentiated asteroids.

2. Methods and Materials

2.1 Sample Description and Distribution

Details of Bunburra Rockhole's textural features, mineralogy, mineral chemistry and chronology are described elsewhere (Towner et al., 2010, Jourdan et al., 2014; Sanborn and Yin, 2014, 2016; Spivak-Birndorf et al., 2015; Sanborn et al., 2016), therefore we only briefly review the important features here. Bunburra Rockhole is a brecciated, basaltic achondrite, with fine- and medium-grained basaltic clasts embedded in a coarse-grained, basaltic matrix. The fine-grained clasts have either basaltic (lathy plagioclase and pyroxene) or granulitic (equilibrated with multiple triple junctions) texture, with both sometimes occurring within the same clast. This texture is consistent with typical brecciated eucrite textures. Modally, Bunburra Rockhole is broadly basaltic with plagioclase (52.5 vol%) and pyroxene (41.4 vol%) comprising the main minerals. Minor and trace components include silica, sulfides, ilmenites, phosphates, and μm-sized zircons.

A 1.81g, somewhat fusion-crusted, piece of Bunburra Rockhole, measuring a little over 2 cm in long dimension, was allocated to the OU for oxygen isotope analyses in 2013. This sample was cut into 3 smaller pieces, labeled A, B, and C. Pieces A and C were further partitioned to analyse clasts of different grain sizes. Fragment A1 is an extraction from A to specifically sample a coarse-grained clast. Piece C was divided into two fragments, C/A and C/B, which were further split. Although each aliquot has a dominant grain size, obtaining material of a single texture was difficult due to the intermixed nature of the breccia and, thus, each aliquot contains some unknown, but small, amount of mixed lithology. Six pieces in chip (A and B) and powder form (A1, C/A/1, C/A/2, C/B/3) were sent to Fordham University for bulk chemical analysis. The oxygen isotope composition was not determined for one of the chips (B). Two pieces (A/1 and C/A/2) were sent to UC Davis for Cr-isotope measurements. A second, fusion-crust free chip weighing 1 g was extracted from the main mass and sent to the Franklin and Marshall College X-ray Laboratory for analysis for bulk major elements. No single piece had all analyses carried out on it, however, C/A/1 and C/A/2, which come from the same subsample of the original piece (1.81g) have had all analyses when combined.

2.2 Methodologies

2.1.1 Computed Tomography

The two main masses were scanned in the Natural History Museum in London, UK using a cone beam projection HMXST 225 system and reconstructed using CT-PRO 2.0 (Metris X-Tek, Tring, UK). Analysis of the resulting scans was carried out using Blob3D (Ketcham, 2005), and VG Studio Max 2.0 (Volume Graphics, Heidelberg, Germany). Data volumes for a given scan are in the range 50-70 GB, and voxel size on the order of ~30 μm^2.

2.1.2 Stable isotopes

2.1.2.1 Oxygen isotopes

Oxygen isotope analysis was carried out at the Open University using an infrared laser-assisted fluorination system (Miller et al., 1999; Greenwood et al., 2014). All analyses were obtained on approximately 2 mg whole rock aliquots drawn from larger homogenized sample powders (see below). Oxygen was released from the sample by heating in the presence of BrF_5. After fluorination, the oxygen gas released was purified by passing it through two cryogenic nitrogen traps and over a bed of heated KBr. Oxygen gas was analyzed using a MAT 253 dual inlet mass spectrometer. Published analytical precision (2σ) for our system, based on replicate analysis of international (NBS-28 quartz, UWG-2 garnet) and internal standards, is approximately ±0.08‰ for $\delta^{17}O$; ±0.16‰ for $\delta^{18}O$; ±0.05‰ for $\Delta^{17}O$ (Miller et al., 1999). Analytical precision, 2σ. based on 39 repeat analyses of our internal obsidian standard (Table 2), is: : ±0.05 for $\delta^{17}O$; ±0.09 for $\delta^{18}O$; ±0.02 for $\Delta^{17}O$. All sample powders analyzed in this study were prepared by crushing whole rock chips with a mass of between 30 mg and 400 mg. Details of the exact mass for each sample are given in Table 1. Sample powders were prepared at the Open University and were crushed to a fine powder in an agate pestle and mortar. The precision (Table 2) quoted for individual fractions separated from Bunburra Rockhole is based on replicate analyses. However, in many cases, due to the small size of the individual clasts, it was only possible to run a single analysis for an individual lithology. In such cases (N=1, Table 2) 2σ values could not be calculated. Also included in table 2 are values for standard error on the mean (SEM), which provides a measure of accuracy.

Oxygen isotopic analyses are reported in standard δ notation, where $\delta^{18}O$ has been calculated as: $\delta^{18}O = [(^{18}O/^{16}O)_{sample}/ (^{18}O/^{16}O)_{ref} - 1] \times 1000$ (‰) and similarly for $\Delta^{17}O$ using the $^{17}O/^{16}O$ ratio (where ref is VSMOW: Vienna Standard Mean Ocean Water). $\Delta^{17}O$, which represents the deviation from the terrestrial fractionation line, has been calculated using a linearized format (Miller, 2002), $\Delta^{17}O = 1000 \ln(1 + \delta^{17}O/1000) - \lambda 1000 \ln(1 + \delta^{18}O/1000)$, where $\lambda = 0.5247$, which was determined using 47 terrestrial whole rock and mineral separate samples (Miller et al., 1999; Miller, 2002).

2.1.2.2 Chromium isotopes

The Cr isotopic composition was measured in two subsamples of Bunburra Rockhole. One 40.52 mg and a 37.55 mg aliquot of homogenized sample powders were used for A/1 and C/A/2, respectively. The sample powders were placed in PTFE Parr digestion capsules along with a 2:1 mixture of ultraclean HF-HNO_3. The PTFE capsules were sealed and placed in a 200°C oven for 96 hours to ensure complete dissolution of refractory phases. After sample dissolution, Cr was separated from the sample matrix using the 3-column chromatography procedure described by Yamakawa et al. (2009). The isotopic composition of the purified Cr fractions was measured using a Thermo *Triton Plus* thermal ionization mass spectrometer at the University of California at Davis.

The Cr fractions were mixed with a silica gel-Al-boric acid activator solution and loaded onto outgassed tungsten filaments. A total of 12 µg of Cr was loaded in equal amounts onto four filaments (i.e., 3 µg on each filament). The sample filaments were bracketed by four filaments loaded with NIST SRM 979 Cr standard.

Each filament analysis consisted of 1200 ratios measured with 8 second integration times. The ^{52}Cr signal was set to 10 V (±15%) for the duration of the measurement. A gain calibration was made at the start of each measurement and a baseline and amplifier rotation was completed between each block of 25 ratios. Uncertainties for the reports $\varepsilon^{54}Cr$ measurements are the external reproducibility of the $^{54}Cr/^{52}Cr$ ratio of the four samples filaments. The external reproducibility of the four bracketing standard filaments is included and propagated into the total error.

The isotopic composition ($^{54}Cr/^{52}Cr$) is expressed as parts per 10,000 deviation (epsilon notation) from the measured NIST SRM 979 terrestrial standard. Mass fractionation correction was made using an exponential law and a normalization ratio of $^{50}Cr/^{52}Cr = 0.051859$ (Shields et al., 1966).

2.1.3 Bulk Chemistry

2.1.3.1 Inductively Coupled Plasma Mass Spectrometry (ICP-MS)

Bulk chemical analyses of Bunburra Rockhole were performed on powders and chips (Table 1) of the rock. Depending on the size of each sample we analyzed a variety of numbers of replicates for each. Sample designations, number of replicates, and the mass (mg) of each aliquot are as follows: sample A (n=4, 86.2, 89.7, 83.1, 57.2), sample B (n=6, 88.0, 83.3, 88.6, 90.7, 90.2, 74.8), sample C/A/1 (n=1, 23.8), sample C/B/3 (n=1, 27.4). Dissolution and ICP-MS analyses are based on a matrix-matching scheme (see Friedrich et al., 2003 and references therein). In short, each sample aliquot was ground to <100 mesh in a clean agate mortar and pestle. Those powders were placed in Teflon bombs with 1 mL HF and 5 mL HNO_3 and placed in a microwave digestion system. The resulting solution is taken to incipient dryness in Teflon beakers on a specially-constructed drybath incubator at 75°C. $HClO_4$ is then added and again the solution is taken to incipient dryness at 75°C. The samples are then taken up to a total of 50 mL of ~1% HNO_3 solution after adding internal standards (Be, Rh, In, Tl) used to correct for potential mass-dependent drift during ICPMS analysis. These solutions were used for trace element analysis; fivefold dilutions of portions of those solutions were used for major element analyses akin to the method of Wolf et al. (2012). We used a Thermo Scientific X Series II ICPMS for all analyses. During ICPMS analysis, the Allende Reference Standard Meteorite (Jarosewich et al., 1987), USGS basaltic standards BIR-1 and BCR-1 and the NIST 688 basalt standard were used for an external calibration scheme for quantification of

the individual elemental analytes. Standards and procedural blanks were digested using the same method outlined above.

2.1.3.2 X-ray Fluorescence

The Franklin & Marshall College X-ray laboratory contains a PANalytical 2404 X-ray fluorescence vacuum spectrometer equipped with a PW2540 X-Y sample handler. It utilizes a 4kW Rh super sharp X-ray tube. Precisely 0.4 grams of rock powder is homogenized with 3.6 grams of lithium-tetraborate and melted in a 95%Pt-5%Au crucible. The molten material is transferred to a 95%Pt-5%Au casting dish and quenched to produce a glass disk that is used for analysis of Na_2O, MgO, Al_2O_3, SiO_2, P_2O_5, K_2O, CaO, TiO_2, MnO and Fe_2O_3. Working curves based on between 30 and 50 data points for each element are determined through analysis of geochemical rock standards (Abbey, 1983; Govindaraju ,1994), and elemental interferences are taken into account. Results are calculated and presented as weight percent oxide, with all Fe determined as Fe_2O_3. Data reported in Table 2 have been recalculated as elemental abundance in mg/g. Loss on ignition is determined by heating an exact aliquot of the sample at 950 °C for one hour. In addition, data for V, Cr, Ni, Zr and Sr are reported as µg/g. These elements were measured on the same glass disks on which the major element were determined. Similar standardization is done as for major elements. The Rh Compton peak is utilized for mass absorption corrections where appropriate. The precision of the XRF procedure is demonstrated through analyses of replicate samples of a single rock, and accuracy is established through repeat analyses of USGS standard rock BHVO-2 (Hawaiian basalt). Additional details of the Franklin & Marshall College X-ray Laboratory instrumentation and analytical protocols can be found at: http://www.fandm.edu/earth-environment/laboratory-facilities/xrf-and-xrd-lab and as a PDF file available in the supplemental data.

3. Results

3.1 Computed tomography

Figure 1 shows a single horizontal CT scan through one of the Bunburra Rockhole stones. The brecciated nature is evident down to a scale of tens of microns. The three grainsize lithologies are discernable and the density contrast between plagioclase (dark grey) and pyroxene (light grey) illustrates the textural relationship between those minerals. High density material (white) is very rare in the scans with only small areas randomly distributed through the Bunburra Rockhole texture. The flip book (movie created of individual tomographic slices) for the largest Bunburra Rockhole sample reveals that the lithologies are heterogeneously distributed through the rock with some areas exhibiting a single lithology.

3.2 Stable isotopes

3.2.1 Oxygen isotopes

The oxygen isotopic compositions of 22 distinct sub-samples (42 replicate analyses) of Bunburra Rockhole are shown in figure 2 and listed in Table 2. The mean $\Delta^{17}O$ and $\delta^{18}O$ values of the complete dataset are -0.134 ± 0.041‰ (-0.186 to -0.091 ‰) and 3.992 ± 0.207‰ (3.744 to 4.233‰) respectively (this study combined with data from Benedix et al., 2013). This slight shift to more positive $\delta^{18}O$ and less negative $\Delta^{17}O$ values remains significantly different from the HED mean $\Delta^{17}O$ value of -0.240 ± 0.014 (Greenwood et al., 2016), which is also shown on the figure. The variation in Bunburra Rockhole shows more than three times the level of oxygen isotope heterogeneity in $\Delta^{17}O$ in the HEDs. The data from Table 2 are plotted in Figure 2 by grain size of each aliquot. It is noteworthy that, although the coarse-grained fraction shows a tendancy to more negative $\Delta^{17}O$ values, the texture does not correlate well with oxygen isotopic composition. The five fragments (A, A/1, C/A/1, C/A/2 and C/B/3; figure 2) for which we also have bulk chemistry cluster around a much tighter mean $\Delta^{17}O$ of -0.133 ± 0.016‰, with $\delta^{18}O$ values at the upper end of the range for Bunburra Rockhole (4.080 ± 0.15‰). Cr isotopes were measured on subsamples A1 and C/A/2 (2 replicate analyses each, see Cr results below) and have average $\Delta^{17}O$ and $\delta^{18}O$ of -0.134 ± 0.007‰ and 4.029 ± 0.037‰.

3.2.2 Chromium isotopes

Figure 3 shows the $\Delta^{17}O$-$\varepsilon^{54}Cr$ isotope space for a number of different meteorite groups (Fig 3a) as well as the detailed region that includes eucrites, other anomalous basaltic achondrites and Bunburra Rockhole (Fig. 3b). The measured $\varepsilon^{54}Cr$ for sample A/1 is -0.37 ± 0.11 and for C/A/2 is -0.35 ± 0.08, which are identical within error. These values are resolvably different from the average $\varepsilon^{54}Cr$ range observed in eucrites of -0.7ε (Figure 3b), but overlap the $\varepsilon^{54}Cr$ observed in angrites of -0.36 ± 0.07 (Trinquier et al., 2007). Bunburra Rockhole is identical, within error, to Asuka 881394 (Sanborn and Yin, 2014) in $\Delta^{17}O$-$\varepsilon^{54}Cr$ isotope space.

3.3 Bulk Composition

3.3.1 Bulk Major elements

Bulk major and minor elements measured by ICP-MS and X-ray fluorescence are listed in Table 3. The values for Piece A and B were analyzed 4 times each and are statistically robust. They can be compared to Piece SM, which was measured by XRF using a more representative sample (400 mg which was homogenized from 1 gram of material sampling all grain sizes of Bunburra Rockhole). Bulk major elements were measured for the smaller pieces C/A/1 and C/B/3, but, based on large variations, it is clear that the samples were not homogenous in their distribution of minerals. The average major (Al, Ca, Mg) and minor (Ti, Cr) element composition of Bunburra Rockhole is

shown in Figure 4 compared to literature data for basaltic and cumulate eucrites, and other anomalous mafic achondrites. Na and K (Table 3) from the XRF data are higher than the ICP-MS results for these elements. We follow the treatment of Mittlefehldt et al. (2013) in dealing with this – weighting the XRF data for Na and K by ½ when calculating the mean. We calculated the average bulk composition by weighting our XRF and ICP-MS analyses by the mass of sample analyzed. Thus, the smaller, possibly non-representative, chips used for ICP-MS analyses have a lesser effect on the bulk average. The Mg content of Bunburra Rockhole is at the low end of the range for main-group basaltic eucrites, and slightly higher than for Nuevo-Laredo-group eucrites. The bulk rock mg# (molar 100MgO/[MgO+FeO]) of Bunburra Rockhole is 37.3 compared to ranges of 35.8-42.0 and 32.5-33.0 for main-group and Nuevo-Laredo-group basaltic eucrites. Other major and minor element concentrations are similar to those of main-group basaltic eucrites although Ca is a little on the low side and Ti is a little on the high side of the ranges (Fig. 4).

3.3.2 Bulk Trace elements

Bulk trace elements for all pieces of Bunburra Rockhole studied here are listed in Table 4.

Rare Earth Elements Bulk rare earth elements (italicized in Table 4) show a relatively flat pattern with a slight negative Eu anomaly (average Eu/Eu = 0.9) for all samples, except piece C/B/3, which has no Eu anomaly (Eu/Eu* = 1.0), falling within the range of concentrations of the basaltic and polymict eucrites (Mittlefehldt, 2015) (Fig 5). Overall concentrations range from ~10× to ~14× CI, except for piece C/A/2 (not shown on figure), which has a REE pattern that is more similar to cumulate eucrites. This is most likely due to the fact that this sample is small and the result is dominated by an unrepresentative mineral mode. These analyses overlap earlier analyses of REE that were measured in specifically more coarse grain size fractions of Bunburra Rockhole (Spivak-Birndorf et al., 2015).

Compositional trends Bulk trace elements for Bunburra Rockhole are plotted in figures 6 (lithophile elements) and 7 (siderophile and chalcophile elements) in order of increasing volatility. The lithophile elements have a pattern that overlaps basaltic and polymict, but is distinct from cumulate, eucrites, at roughly 10× CI until around T = 1450K (i.e. ~ 1177˚C) when the concentrations fall off in a spiky pattern, although there are only 3 elements with 50% condensation temperatures less than 1450K. Siderophile element concentrations in Bunburra Rockhole are low, ranging over three orders of magnitude but generally less than CI. The overall pattern is similar to what is seen in the eucrites. There are some differences in abundance: Te is significantly and Cu is slightly depleted in Bunburra Rockhole than in eucrites, while As is considerably enriched.

4. Discussion

4.1 Anomalous nature

In this study we set out to investigate the anomalous nature of Bunburra Rockhole to sort out its provenance. The calculated orbit for Bunburra Rockhole showed that it came from an asteroid in an Aten-type orbit (Bland et al., 2009; Spurný et al., 2012). Using a probabilistic orbital evolution model (Bottke et al., 2002), Bland et al. (2009) showed that Bunburra Rockhole originated from the innermost main belt, interior to 4 Vesta and the core Vestoid family (Zappala et al., 1995). This was the first indication that it was anomalous. The oxygen isotope data (Table 2; Fig 2-3) also showed that Bunburra Rockhole had anomalous characteristics (Bland et al., 2009). Our data significantly extend that initial oxygen isotope study, and confirm the anomalous (and highly variable) nature of Bunburra Rockhole oxygen. Chromium isotopes also support the anomalous nature of Bunburra Rockhole.

In contrast, mineralogically and chemically (based upon bulk and mineral trace element patterns (Spivak-Birndorf et al., 2015)), Bunburra Rockhole appears identical to the basaltic eucrites. The modal mineralogy is very similar to average eucrite modes (Mittlefehldt, 2015), with the exception that the plagioclase to pyroxene ratio is reversed. Plagioclase and pyroxene compositions (both in major and minor elements) overlap compositions of those minerals in eucrites (Spivak-Birndorf et al., 2015). So this begs the question, how can a rock that looks in every way like a basaltic eucrite, down to mineral chemistry (major and trace) have such a different isotopic composition and orbit? We explore three hypotheses in an effort to explain Bunburra Rockhole's different bulk isotopic composition.

4.1.1 Mixing with other source(s)

In the initial study (Bland et al., 2009), it was found there was no correlation between grain size and oxygen isotopic composition, but the data fell between the eucrite and angrite fractionation lines (fig 2b, 2009 data points). Additional aliquots of Bunburra Rockhole (fig. 2b; 2012 and 2013 data points) were analyzed to assess whether a mixing line between the two groups could be found. The distribution of analyses is not linear, which implies it is not simple mixing, as is the case for CM chondrites (Clayton, 1999). The fact that we do not observe a mixing line between eucrite and a possible contaminant (either angrite or ordinary chondrite) indicates that contamination cannot account for the oxygen isotope variability within Bunburra Rockhole. If the contaminant were an ordinary chondrite (OC), as is the case for JaH 556 (Janots et al., 2012), the oxygen isotopic composition would shift $\Delta^{17}O$ toward the terrestrial fractionation line, which is what we see with Bunburra Rockhole (Fig 2). However, it was shown in Sanborn et al (2016) that mixing between

ordinary chondrites (and other known chondrite sources) and normal eucrite end members would not pass through Bunburra Rockhole point in the $\Delta^{17}O$-$\varepsilon^{54}Cr$ space, which effectively rules out a mixing scenario. Additionally, unlike JaH 556, which clearly has clasts of exotic material embedded in the main meteorite type, we do not see any exotic clasts in Bunburra Rockhole on the cut or broken surfaces. Further, a significant fraction (>10%) of contaminant material would be required to affect the oxygen isotopic composition. Thus, any OC material present would likely be visible in the CT scans due to the density differences between OC (3 to 3.7 g/cm3) and basalt (2.8 to 3 g/cm3) as well as the presence of metallic grains in OC. Although CT scanning cannot easily distinguish between the silicates in meteorites, the density of metallic particles is easily seen, even in melted OC (Benedix et al., 2008). Micro-CT of both the 150g and 174g Bunburra Rockhole masses did not reveal any contaminant with a density contrast at scales >30µm (Towner et al., 2010).

The bulk major and trace element concentrations and patterns are also inconsistent with mixing. The oxygen data occupy the $\Delta^{17}O$ space between the HED and angrite fractionation lines. Could mixing between eucrites and angrites be an explanation for the anomalous oxygen? To achieve a Bunburra Rockhole oxygen composition would require a ~70:30 mix of angrite:eucrite. Although it would be harder to distinguish angrite contamination with CT, due to the fact that they are both achondritic and, thus, do not have substantial density differences, the presence of angrite material would have a significant impact on bulk and mineral major element chemistry, which is not seen. Angrites have less SiO_2 and Na_2O compared to eucrites (McCoy et al., 2006; Keil 2012). The difference in SiO_2 (35-40 wt% for angrites vs 45-50 wt% for eucrites) leads to extreme differences in viscosity (2.06 Pa s vs 16.1 Pa s) and a lower liquidus temperature (1155˚C vs 1185˚C). Na_2O in angrites is at trace element levels (average <0.03 %; Keil, 2012), while in basaltic and polymict eucrites the average value is 0.45 wt% (Mittlefelhdt, 2015). In addition, the molar Fe/Mn ratio in angrite pyroxenes falls between 90 to 130 (Papike et al. 2003), while for eucrite pyroxenes ranges from 30 to 38. These differences would produce a bulk chemistry closer to angrite than is seen in Bunburra Rockhole. Bunburra Rockhole, with an average bulk SiO_2 of ~50 wt%, Na_2O of ~0.42 wt% and a pyroxene Fe/Mn of 33 (Spivak-Birndorf et al., 2015), falls squarely within the eucrite range.

Finally, the chalcophile and siderophile element concentrations do not support the presence of a contaminant (Fig. 7). Although the abundances for some elements (e.g. Pt, Ir, and As) are higher than basaltic eucrites (Dale et al., 2012), it is not consistent with contamination by chondritic material. Using the same calculation as presented above for oxygen isotope compositions, Figure 8 reveals that adding roughly 10% of ordinary chondritic (H, L, or LL) siderophile elements to an average eucrite (Stannern) does not explain the increase in these elements. If OC metal and/or

sulfide compents had been introduced into Bunburra Rockhole, there would be a smooth increase in the chalcophile and siderophile element contents of Bunburra Rockhole. The increased abundance of Pt, Ir and As must be controlled by something else. It is most likely due to heterogeneous cooling of the parent body, which could be due to a small size.

4.1.2 Heterogeneous Parent Body

Wiechert et al. (2004) hypothesized that 4 Vesta may not have homogenized isotopically. This was based on analysis of oxygen isotopes in a number of howardites, eucrites and diogenites. In their study, all but a few anomalous eucrites, had oxygen isotopic compositions with similar $\Delta^{17}O$ values, indicating they come from the same body. Wiechert (2004) postulated that the anomalous samples could also be from 4 Vesta if it had not experienced full magma ocean melting, as proposed by (Righter and Drake, 1997). The major argument against a heterogenous Vesta is based on both the oxygen and chromium isotopic compositions. The eucrite parent body fractionation line is based on the analyses of a large number of those meteorites. There is no a priori reason to think that each individual normal eucrite originated in the same area of the parent body - the samples include unbrecciated, polymict, monomict, and cumulate eucrites. In addition to eucrites, the diogenites, which are pyroxenites and, therefore, likely sample a different, deeper part of the parent body, have identical $\Delta^{17}O$ to eucrites (Greenwood et al., 2014). Given this range of petrologic types, the simplest explanation is that the oxygen was homogenized in the body before eucrite formation, and, thus, Bunburra Rockhole is not sampling an unknown, heterogenous area of 4 Vesta. The $\varepsilon^{54}Cr$ isotope data support and strengthen the argument against heterogeneity on Vesta. Sanborn et al (2016) have shown that normal HEDs have a very narrow range of $\varepsilon^{54}Cr$ within errors of the measurements. Whereas the anomalous eucrites, including Bunburra Rockhole, are clearly outside the normal range. Because $\varepsilon^{54}Cr$ isotopic anomalies could only be created by stellar nucleosynthetic sources (*c.f.* Wasserburg et al., 2015 and references therein), the grouping of planetary materials in the $\Delta^{17}O$-$\varepsilon^{54}Cr$ space (see Fig. 3, and Schmitz et al., 2016) indicates distinct isotopic reservoirs in the protoplanetary disk from which planetary materials accreted from. The fact that both isotope systems plot away from the normal eucrite and angrite groups indicates that Bunburra Rockhole is not simply an anomalous piece of 4 Vesta.

4.1.3 A new differentiated parent body

The third possibility is that Bunburra Rockhole samples a different parent asteroid with a basaltic crust that had a very similar geologic history to 4 Vesta. This scenario is the most reasonable given the O- and Cr-isotopic compositions, and its unusual orbit; however, this theory was questioned due to the similarity of mineral chemistry (pyroxene Fe/Mn vs Fe/Mg) and bulk trace element features

which matched bulk eucrite data almost exactly (Spivak-Birndorf et al., 2015). Initial concerns related to the bulk composition are alleviated with our new, higher resolution bulk chemical data. As discussed above and shown in Figure 4, Bunburra Rockhole generally lies outside the field of basaltic eucrites and does not fit with cumulate eucrites at all. There is some overlap with the Stannern and Nuevo Laredo trends, but it is not consistent across all elements. On these plots are also shown data for a number of anomalous (or ungrouped) basaltic achondrites, some of which have oxygen isotopes similar to Asuka (A-)881394 (ungrouped A) and others with oxygen isotopes similar to Pasamonte (ungrouped P).

Because the oxygen and chromium isotope compositions of Bunburra Rockhole are so similar to Asuka 881394 (A-881394), it would be of interest to explore this relationship further. These two meteorites are quite different texturally. Whereas Bunburra Rockhole has variable grain sizes and is clastic in nature (Spivak-Birndorf, et al., 2014), A-881394 appears to be a coarse-grained, cumulate-textured rock (Nyquist et al., 2003). The mineralogy in both meteorites is primarily plagioclase and pyroxene, but the mineral chemistry of plagioclase, in particular, is difficult to reconcile if the two sample the same asteroid. A-881394 contains plagioclase ($An_{98;}$ Nyquist et al., 2003) that is more calcic than found in basaltic or cumulate eucrites (An_{75-91}) (Mittlefehldt et al., 2016), or Bunburra Rockhole (An_{87-90}; Spivak-Birndorf et al., 2014). At this point, the relationship between these two meteorites is unclear and other studies are needed to strengthen any ties or prove they are not related. This is beyond the scope of this study and we will focus on the evolution of Bunburra Rockhole for the rest of this paper.

We suggest that Bunburra Rockhole samples a new differentiated asteroid, distinct in O- and Cr-isotopic composition to 4 Vesta, and with subtle but real differences in bulk composition. However, the fact that bulk compositions are so similar indicates a similar precursor source, perhaps suggesting that the Bunburra Rockhole parent body and 4 Vesta sampled a similar formation zone in the early Solar System. The close match in mineralogy and mineral chemistries indicates similar parent body petrogenetic histories. The primary material must have experienced heating and melting, but perhaps not full differentiation, under similar redox, pressure and temperature conditions. The bulk chemistry of basaltic rocks on Earth identifies the physicochemical conditions of different sources. It seems logical to expect that similar compositions/ages could be interpreted as comparable bulk composition undergoing the same process to end at very similar compositions and mineralogies. Paradoxically, Bunburra Rockhole oxygen is significantly more variable (at the scale of a single stone, a range of 4× that of the HED and angrite parent body fractionation lines).

The most logical explanation is that the precursor body was likely smaller than 4 Vesta. Because a smaller body will have a larger surface area to volume ratio, it will cool more quickly. For a body

with a diameter 100km smaller than Vesta, cooling would happen ~25% faster. This is consistent with the variations we see in oxygen isotopic composition as well as more variable trace siderophile element compositions, where it is clear that equilibration after differentiation hasn't been reached. While we can not estimate the exact body size in this study, it couldn't have been much smaller than 4 Vesta, because rare earth element patterns and bulk major elements indicate similar levels of partial melting.

Taken together, these data indicate that there may be hidden diversity in igneous meteorites, pointing to a larger number of discrete parent bodies, and that the igneous history of planetesimals in the early system may be more complex than previously thought.

5. Conclusion

We conclude that Bunburra Rockhole samples a new differentiated parent body that isn't 4 Vesta. This is based on a lack of evidence for contamination with any chondritic sources. In addition, the chemical composition indicates that contamination with a non-chondritic source (most likely angrites) is unlikely. The major element compositions of Bunburra Rockhole are only slightly different, while trace elements (in particular rare earth elements) are identical to eucrites. Oxygen and chromium isotope compositions plot well away from the eucrite and angrite parent bodies, consistent with Bunburra Rockhole's origin on a separate differentiated body.

This differentiated body had an Aten type orbit, almost entirely within the orbit of the Earth. Modeling has shown that its orbit most likely evolved from the inner most asteroid belt. Whether it formed closer to the sun and was flung to the inner belt is unknown, but given the similarity of bulk major and trace element (i.e. volatility) compositions between Bunburra Rockhole and the basaltic/polymict eucrites, it seems possible that it formed in a similar region of space as 4 Vesta. It could have experienced a similar magmatic history (although the wider range in oxygen isotope data for Bunburra Rockhole means that a full body magma ocean scenario is unlikely).

Bunburra Rockhole samples the same oxygen and chromium isotope space as Asuka 881394. Mineral chemistry features imply they can not be from the same asteroid. This means that there could be a second differentiated body that formed in the same region at about the same time as the parent body of Bunburra Rockhole.

Acknowledgements

The authors would like to acknowledge a number of funding bodies for support of this work: Curtin Research Fellowship (CRF140045, GKB); Australian Research Council Laureate Fellowship (PAB); NASA Emerging Worlds (NNX15AL69G, DWM and QZY), NASA Cosmochemistry (NNX14AM62G, QZY) and Emerging Worlds

(NNX16AD34D, QZY); . This manuscript was greatly enhanced by detailed reviews from Nicole Lunning, Luigi Folco, an anonymous reviewer and AE Frederic Moynier.

6. References

Abbey S. 1983. Studies in "standard samples" of silicate rocks and minerals, 1969-1982. *Geological Survey of Canada*. Paper 83-15:1-114

Anders E. and Grevesse N. (1989) Abundances of the elements: Meteoritic and solar. *Geochimica et Cosmochimica Acta* **53**, 197–214.

Benedix G. K., Bland P. A., Greenwood R. C., Franchi I. A., Friedrich J. M. and Towner M. C. (2013) Where Did Anomalous Basaltic Meteorites Get Their Oxygen Anomaly? the Case of Bunburra Rockhole. *Meteoritics and Planetary Science* **48**, A55–A55.

Benedix G., Benedix G. K., Ketcham R. A., Ketcham R., Wilson L., McCoy T., McCoy T. J., Bogard D., Bogard D. D., Garrison D., Garrison D. H., Herzog G., Herzog G. F., Xue S., Klein J. and Middleton R. (2008) The formation and chronology of the PAT 91501 impact-melt L chondrite with vesicle metal sulfide assemblages. *Geochimica et Cosmochimica Acta* 72, 2417–2428.

Binzel R. P. and Xu S. (1993) Chips off of asteroid 4 Vesta - Evidence for the parent body of basaltic achondrite meteorites. *Science (ISSN 0036-8075)* **260**, 186–191.

Bland P. A., Bland P. A., Spurný P., Spurny P., Towner M. C., Towner M. C., Bevan A. W. R., Bevan A. W. R., Singleton A. T., Singleton A. T., Bottke W. F., Bottke W. F., Greenwood R. C., Greenwood R. C., Chesley S. R., Chesley S. R., Shrbený L., Shrbeny L., Borovicka J., Borovička J., Ceplecha Z., Ceplecha Z., Mcclafferty T. P., McClafferty T. P., Vaughan D., Vaughan D., Benedix G. K., Benedix G. K., Deacon G., Deacon G., Howard K. T., Howard K. T., Franchi I. A., Franchi I. A., Hough R. M. and Hough R. M. (2009) An Anomalous Basaltic Meteorite from the Innermost Main Belt. *Science* **325**, 1525–1527.

Bland P. A., Spurny P., Bevan A. W. R., Howard K. T., Towner M. C., Benedix G. K., Greenwood R. C., Shrbeny L., Franchi I. A., Deacon G., Borovicka J., Ceplecha Z., Vaughan D. and Hough R. M. (2012) The Australian Desert Fireball Network: a new era for planetary science. *Australian Journal of Earth Sciences* **59**, 177–187.

Bottke W. F., Morbidelli A., Jedicke R., Petit J. M., Levison H. F., Michel P. and Metcalfe T. S. (2002) Debiased Orbital and Absolute Magnitude Distribution of the Near-Earth Objects. *Icarus* **156**, 399–433.

Bottke W. F., Nesvorný D., Grimm R. E., Morbidelli A. and O'Brien D. P. (2006) Iron meteorites as remnants of planetesimals formed in the terrestrial planet region. *Nature* **439**, 821–824.

Burbine, T.H., McCoy, T.J., Meibom, A., Gladman, B., Keil, K., (2002) Meteorite Parent Bodies: Their number and identification. In Asteroids III (eds. Bottke W.F. et al) Univ. Arizona Press, Tucson. pp 653-667.

Clayton R. N. (1999) Oxygen isotope studies of carbonaceous chondrites. *Geochimica et Cosmochimica Acta* **63**, 2089-2104.

Clayton R. N. and Mayeda T. K. (1984) The oxygen isotope record in Murchison and other carbonaceous chondrites. *Earth and Planetary Science Letters* **67**, 151–161.

Clayton R. N. and Mayeda T. K. (1996) Oxygen isotope studies of achondrites. *Geochimica et Cosmochimica Acta* **60**, 1999–2017.

Clayton R. N., Grossman L. and Mayeda T. K. (1973) A Component of Primitive Nuclear Composition in Carbonaceous Meteorites. *Science* **182**, 485–488.

Dale C. W., Burton K. W., Greenwood R. C., Gannoun A., Wade J., Wood B. J. and Pearson D. G. (2012) Late Accretion on the Earliest Planetesimals Revealed by the Highly Siderophile Elements. *Science* **336**, 72–75.

Franchi, I.A. (2008) Oxygen isotopes in asteroidal meteorites. In Reviews in Mineralogy & Geochemistry 68, 345-397

Friedrich J. M., Wang M.-S. and Lipschutz M. E. (2003) Chemical studies of L chondrites. V: compositional patterns for 49 trace elements in 14 L4-6 and 7 LL4-6 falls. *Geochimica et Cosmochimica Acta* **67**, 2467–2479.

Govindaraju, K. 1994. 1994 compilation of working values and sample description for 383 geostandards. *Geostandards Newsletter* 18 (S1):1-158

Gradie J., and Tedesco, E. (1982) Compositional structure of the asteroid belt. Science 216, 1405-1407.

Greenwood R. C., Franchi I. A., Jambon A. and Buchanan P. C. (2005) Widespread magma oceans on asteroidal bodies in the early Solar System. *Nature* **435**, 916–918.

Greenwood R. C., Barrat J.-A., Yamaguchi A., Franchi I. A., Scott E. R. D., Bottke W. F. and Gibson J. M. (2014) The oxygen isotope composition of diogenites: Evidence for early global melting on a single, compositionally diverse, HED parent body. *Earth and Planetary Science Letters* **390**, 165–174.

Greenwood R. C., Burbine T. H., Miller M. F. and Franchi I. A. (2016) Melting and differentiation of early-formed asteroids: The perspective from high precision oxygen isotope studies. DOI: *10.1016/j.chemer.2016.09.005*.

Grimm, R.E., McSween, H.Y., (1993) Heliocentric zoning of the asteroid belt by aluminum-26 heating. Science 259, 653-655.

Hevey P. J. and Sanders I. S. (2006) A model for planetesimal meltdown by 26Al and its implications for meteorite parent bodies. *Meteoritics and Planetary Science* **41**, 95-106.

Janots E., Gnos E., Hofmann B. A., Greenwood R. C., Franchi I. A., Bermingham K. and Netwing V. (2012) Jiddat al Harasis 556: A howardite impact melt breccia with an H chondrite component. *Meteoritics and Planetary Science* **47**, 1558–1574.

Jarosewich, E., Clarke, R. S., Jr., and Barrows, J. N. (1987) The Allende meteorite reference sample. *Smithsonian Contrib. Earth Sci.* **27**, 1-49.

Jourdan F., Benedix G., Eroglu E., Bland P. A. and Bouvier A. (2014) 40Ar/39Ar impact ages and time-temperature argon diffusion history of the Bunburra Rockhole anomalous

basaltic achondrite. *Geochimica et Cosmochimica Acta* **140**, 391–409.

Keil K. (2010) Enstatite achondrite meteorites (aubrites) and the histories of their asteroidal parent bodies. *Chemie der Erde - Geochemistry*, 1–23.

Keil K. (2012) Angrites, a small but diverse suite of ancient, silica-undersaturated volcanic-plutonic mafic meteorites, and the history of their Parent asteroid. *Chemie der Erde - Geochemistry* **72**, 191–218.

Ketcham R. A. (2005) Computational methods for quantitative analysis of three-dimensional features in geological specimens. *Geosphere* **1**, 32–41.

Lentz R., Scott E. and McCoy T. (2007) Anomalous Eucrites: Using Fe/Mn to Search for Different Parent Bodies. *Lunar Planet. Sci. XXXVIII.* Lunar Planet. Inst., Houston. #1968 (abstr).

McCord T. B., Adams J. B. and Johnson T. V. (1970) Asteroid Vesta: Spectral Reflectivity and Compositional Implications. *Science* **168**, 1445–1447.

McCoy T. J., Ketcham R. A., Wilson L., Benedix G. K., Wadhwa M. and Davis A. M. (2006) Formation of vesicles in asteroidal basaltic meteorites. *Earth and Planetary Science Letters* **246**, 102–108.

Miller M. F., Franchi I. A., Sexton A. S. and Pillinger C. T. (1999) High-precision d17O Isotope Measurements of Oxygen from Silicates and Other Oxides: Method and Applications. *Rapid Communications in Mass Spectrometry* **13**, 1211–1217.

Miller M. F. (2002) Isotopic fractionation and the quantification of ^{17}O anomalies in the oxygen three-isotope system: an appraisal and geochemical significance. *Geochim. Cosmochim. Acta* **66**, 1881–1889.

Mittlefehldt D. (2005) Ibitira: A basaltic achondrite from a distinct parent asteroid and implications for the Dawn mission. *Meteoritics and Planetary Science*. **40**, 665–677.

Mittlefehldt D. W. (2015) Asteroid (4) Vesta: I. The howardite-eucrite-diogenite (HED) clan of meteorites. *Chemie der Erde - Geochemistry* **75**, 155–183.

Mittlefehldt D. W., McCoy T. J., Goodrich C. A. and Kracher A. (1998) Non-chondritic meteorites from asteroidal bodies. *Planetary Materials* **36**, D1–D195.

Mittlefehldt D. W., Greenwood R. C., Peng Z. X., Ross D. K., Berger E. L. and Barrett T. J. (2016) Petrologic and Oxygen-Isotopic Investigations of Eucritic and Anomalous Mafic Achondrites,*Lunar Planet. Sci.* **47**, #1240 (abstr.)

Nyquist L. E., Reese Y., Wiesmann H., Shih C.-Y. and Takeda H. (2003) Fossil 26Al and 53Mn in the Asuka 881394 eucrite: evidence of the earliest crust on asteroid 4 Vesta. *Earth and Planetary Science Letters* **214**, 11.

Papike J. J., Karner J. and Shearer C. (2003) Determination of planetary basalt parentage: A simple technique using the electron microprobe. *American Mineralogist* **88**, 469–472.

Pepin R. O. (1985) Meteorites - Evidence of Martian Origins. *Nature* **317**, 473–475.

Righter K. and Drake M. J. (1997) A magma ocean on Vesta: Core formation and petrogenesis

of eucrites and diogenites. *Meteoritics and Planetary Science* **32**, 929–944.

Sanborn M. E. and Yin Q. Z. (2014) Chromium Isotopic Composition of the Anomalous Eucrites: An Additional Geochemical Parameter for Evaluating Their Origin. *Lunar and Planetary Science Conference* **45**, #2018 (abstr.).

Sanborn, M. E., Yin, Q.-Z. and Irving, A. J. (2014) Isotope Forensics Utilizing $\Delta^{17}O$-$\varepsilon^{54}Cr$ Systematics Provide Supporting Evidence for Differentiated Parent Bodies Overlain by Chondritic Veneers: A Case for the CR Parent Body. 45th Lunar Planet. Sci., #2032 (abstr.), Lunar Planet. Inst., Houston.

Sanborn, M. E. Yin, Q.-Z., and Mittlefehldt, D. W. (2016) The Diversity of Anomalous HEDs: Isotopic Constraints on the Connection of EET 92023, GRA 98098, and Dhofar 700 with Vesta. 47th Lunar Planet. Sci., #2256 (abstr.), Lunar Planet. Inst., Houston.

Schmitz, B., Yin, Q.-Z., Sanborn, M. E., Tassinari, M., Caplan, C. E., and Huss, G. R. 2016. A new type of solar-system material recovered from Ordovician marine limestone. Nature Communications 7:11851

Scott E.R.D. 1979. Origin of iron meteorites. In Asteroids (T. Gehrels, ed.). Univ. of Arizona Press, Tucson. pp 892-925.

Scott E. R. D., Greenwood R. C., Franchi I. A. and Sanders I. S. (2009) Oxygen isotopic constraints on the origin and parent bodies of eucrites, diogenites, and howardites. *Geochimica et Cosmochimica Acta* **73**, 5835–5853.

Shields, W.R., Murphy, T.J., Catanzar, E.J., Garner, E.L., 1966. Absolute isotopic abun- dance ratios and atomic weight of a reference sample of chromium. *J. Res. Nat. Bur. Stand*. Section A-Physics and Chemistry A **70**, 193–197.

Shirai N., Okamoto C., Yamaguchi A. and Ebihara M. (2016) Siderophile elements in brecciated HED meteorites and the nature of projectile materials in HED meteorites. *Earth and Planetary Science Letters* **437**, 57–65.

Spivak-Birndorf L. J., Bouvier A., Benedix G. K., Hammond S., Brennecka G. A., Howard K., Rogers N., Wadhwa M., Bland P. A., Spurný P. and Towner M. C. (2015) Geochemistry and chronology of the Bunburra Rockhole ungrouped achondrite. *Meteoritics and Planetary Science* **50**, 958–975.

Spurný P., Bland P. A., Shrbený L., Borovička J., Ceplecha Z., Singelton A., Bevan A. W. R., Vaughan D., Towner M. C., McClafferty T. P., Toumi R. and Deacon G. (2012) The Bunburra Rockhole meteorite fall in SW Australia: fireball trajectory, luminosity, dynamics, orbit, and impact position from photographic and photoelectric records. *Meteoritics and Planetary Science* **47**, 163–185.

Towner M. C., Duffy C. M., Bland P. A., Spurny P., Spurný P. and Abel R. L. (2010) The Bulk Properties of Bunburra Rockhole: Results of Micro-CT Scan Analysis. *Lunar Planet. Sci.* **41**, #1758 (abstr.) Lunar Planet. Inst., Houston

Trinquier A., Birck J.-L. and Allègre C. J. (2007) Widespread 54Cr Heterogeneity in the Inner Solar System. *ApJ* **655**, 1179–1185.

Wasson J.T. (1990) Ungrouped iron meteorites in Antarctica: Origin of anomalously high

abundance. Science 249, 900-902.

Wasson J. T. and Kallemeyn G. W. (1988) Compositions of Chondrites. *Philosophical Transactions of the Royal Society, A-Mathematical Physical and Engineering Sciences* **325**, 535–544.

Wasserburg, G. J., Trippella, O., Busso, M. (2015) Isotope anomalies in the Fe-Group Elements in meteorites and connections to nucleosynthesis in AGB stars. The Astrophysical Journal 805:7-25.

Weisberg M. K., Smith C., Benedix G., Folco L., Yamaguchi A. and Chennaoui Aoudjehane H. (2009) The Meteoritical Bulletin, No. 95. *Meteoritics and Planetary Science* **44**, 429–462.

Welten K. C., Meier M. M. M., Caffee M. W., Laubenstein M., Nishizumi K., Wieler R., Bland P. A., Towner M. C. and Spurný P. (2012) Cosmic-ray exposure age and preatmospheric size of the Bunburra Rockhole achondrite. *Meteoritics and Planetary Science* **47**, 186–196.

Wiechert U. H., Halliday A. N., Palme H. and Rumble D. (2004) Oxygen isotope evidence for rapid mixing of the HED meteorite parent body. *Earth and Planetary Science Letters* **221**, 373–382.

Wolf S. F., Wang M.-S. and Lipschutz M. E. (2009) Labile trace elements in basaltic achondrites: Can they distinguish between meteorites from the Moon, Mars, and V-type asteroids? *Meteoritics and Planetary Science* **44**, 891-903.

Wolf S. F., Compton J. R. and Gagnon C. J. L. (2012) Determination of 11 major and minor elements in chondritic meteorites by inductively coupled plasma mass spectrometry. *Talanta* **100**, 276–281.

Yamaguchi A., Clayton R. N., Mayeda T. K., Ebihara M., Oura Y., Miura Y. N., Haramura H., Misawa K., Kojima H. and Nagao K. (2002) A New Source of Basaltic Meteorites Inferred from Northwest Africa 011. *Science* **296**, 334-336.

Yamakawa A., Yamashita K., Makishima A. and Nakamura E. (2009) Chemical Separation and Mass Spectrometry of Cr, Fe, Ni, Zn, and Cu in Terrestrial and Extraterrestrial Materials Using Thermal Ionization Mass Spectrometry. *Anal. Chem.* **81**, 9787–9794.

Yurimoto, H., Kuramoto, K., Krot, A.N., Scott, E.R.D., Cuzzi, J.N., Thiemens, M.H., Lyons, J.R. (2007) Origin and evolution of oxygen-isotopic compositions of the solar system. In Protostars and Planets V. (Reipurth, B. Jewitt, D., Keil, K. eds) University of Arizona press, Tucson p.849-862.

Zappalà V., Bendjoya P., Cellino A., Farinella P. and Froeschlé C. (1995) Asteroid families: Search of a 12,487-asteroid sample using two different clustering techniques. *Icarus* **116**, 291–314.

Figure captions

Figure 1. X-ray computed tomographic (CT) slice through the Bunburra Rockhole meteorite. Image is optimized for contrast and brightness to illustrate different lithology types. Scale bar is 10mm.

Figure 2. $\Delta^{17}O$ versus $\delta^{18}O$ for 42 replicate analyses of 22 different pieces of Bunburra Rockhole. Also shown are the fractionation lines (dashed with grey shading indicating 2σ standard deviation for these fractionation lines) for the main groups of differentiated meteorites, the HED and Angrite achondrite meteorites. Different grain size fractions are highlighted (as per legend). Data for the targeted pieces analysed for bulk chemistry here are denoted with stars. These data are from mixed and coarse-grained lithologies. Data for normal eucrites and angrites are from Greenwood et al. (2005, 2014, 2016).

Figure 3. (a) $\Delta^{17}O$ versus $\varepsilon^{54}Cr$ plot showing the systematics of Bunburra Rockhole in comparison with other meteorite groups. Shown are the literature data (diamond symbols) for ureilites, acapulcoites, normal eucrites and diogenites (HEDs), aubrites, enstatite chondrites, martian (SNC) meteorites, ordinary chondrites, and samples from Earth, and the Moon. Note that both $\Delta^{17}O$ and $\varepsilon^{54}Cr$ values have been plotted with 2σ errors. Also shown are the $\Delta^{17}O$-$\varepsilon^{54}Cr$ compositions of the anomalous basaltic achondrites (square symbols): Ibitira, Asuka 881394, Pasamonte, PCA 91007, and NWA 1240. Literature data for $\Delta^{17}O$ values are from Clayton and Mayeda (1984; 1996), and Scott et al. (2009). Literature values for $\varepsilon^{54}Cr$ are from Sanborn and Yin (2014) and Trinquier et al. (2007). (b) Magnified view of the gray region highlighted in panel A.

Figure 4. Binary diagrams for select major (Al, Ca, Mg) and minor (Ti, Cr) element concentrations of Bunburra Rockhole compared to literature data for basaltic and cumulate eucrites, and ungrouped mafic achondrites. Ungrouped (A) are those with oxygen isotopic compositions like that of A-881394, while ungrouped (P) have O isotopic compositions similar to Pasamonte. Although falling outside the basaltic eucrite field (purple field) for all elements, there are no consistent trends with other anomalous samples. Literature data and their sources are given in the on-line supporting information associated with (Mittlefehldt, 2015).

Figure 5. Bulk rare earth element compositions normalized to CI chondrite (Anders and Grevesse, 1989). The shaded areas indicate the ranges of REE in basaltic, polymict and cumulate eucrites. The red and yellow lines are the REE data from Spivak-Birndorf et al. (2015) and our new data are the grey lines as denoted in the legend. The REE for the different pieces of Bunburra Rockhole fall in the middle of the range of basaltic and polymict eucrites. The basaltic eucrites show a much wider array of Eu anomalies, while Bunburra Rockhole has only a slight negative anomaly.

Figure 6. Lithophile elements in Bunburra Rockhole normalized to CI (Anders and Grevesse, 1989). Elements are plotted in order of decreasing condensation temperature to the right. Bunburra Rockhole overlaps the average values for basaltic and polymict eucrites with no significant differences. Basaltic, polymict, and cumulate eucrite data from Mittlefehldt (2015).

Figure 7. Siderophile and chalcophile elements in Bunburra Rockhole normalized to CI (Anders and Grevesse, 1989). Elements are plotted in order of increasing volatility to the right. Basaltic, polymict, and cumulate eucrite data from Mittlefehldt (2015).

Figure 8. Siderophile and chalcophile elements as in Figure 7. Shown here is the average of these elements (including Ni and S) for Bunburra Rockhole (dashed black line) and Stannern (dark grey thick line), a typical eucrite. Also shown are the results of adding 10% of H (dark grey thin line), L (medium grey thin line), and LL (light grey thin line) ordinary chondrite material to Stannern. The diamonds show the range of values of the individual analyses for Stannern (data from Mittlefehldt, 2015; supplemental tables). As discussed in the text, an addition of 10% of OC contaminant would be very noticeable at the trace element level of siderophile elements. The pattern in Bunburra Rockhole is not consistent with contamination with OC materials.

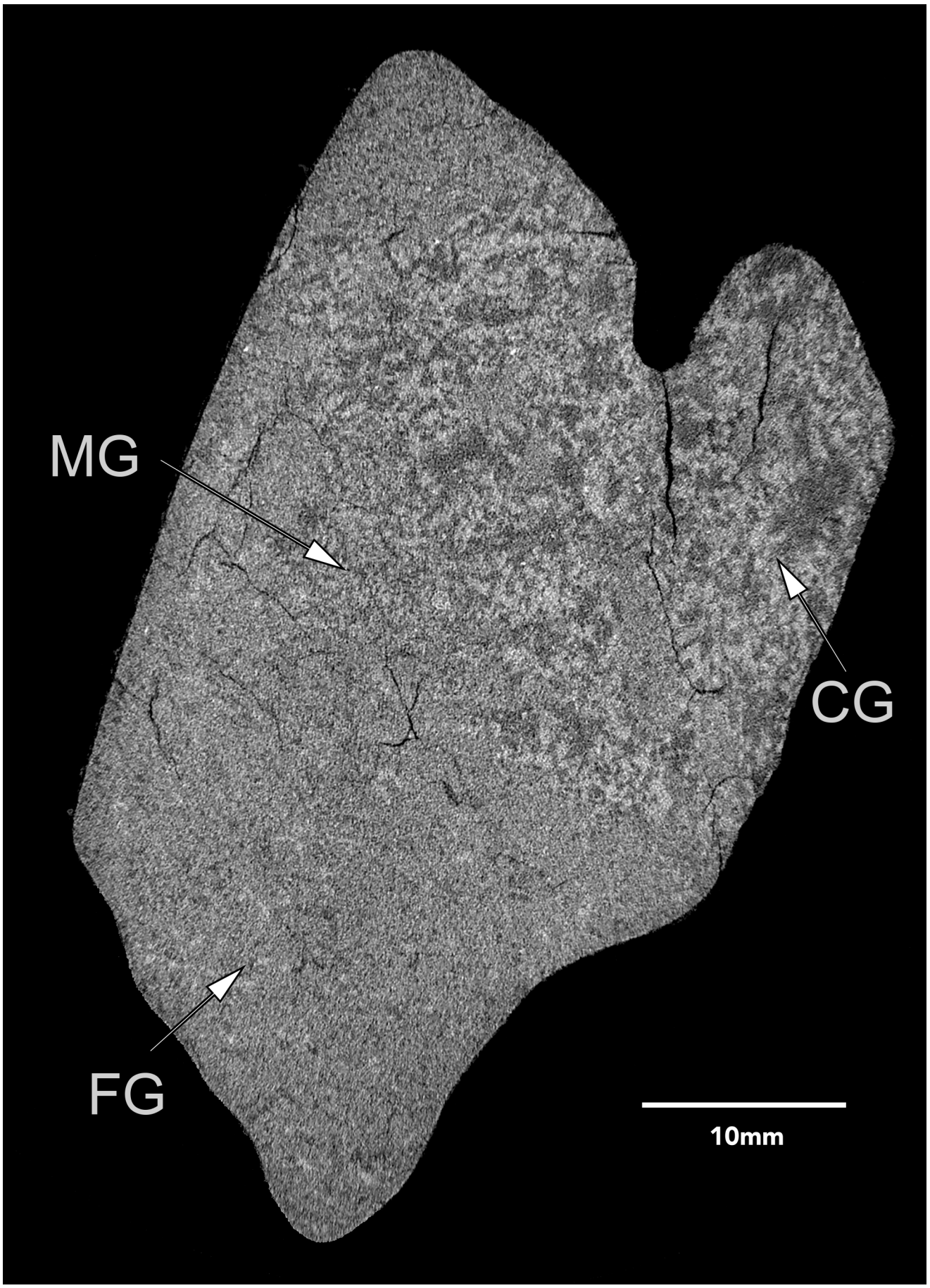

Figure 1

Figure 2

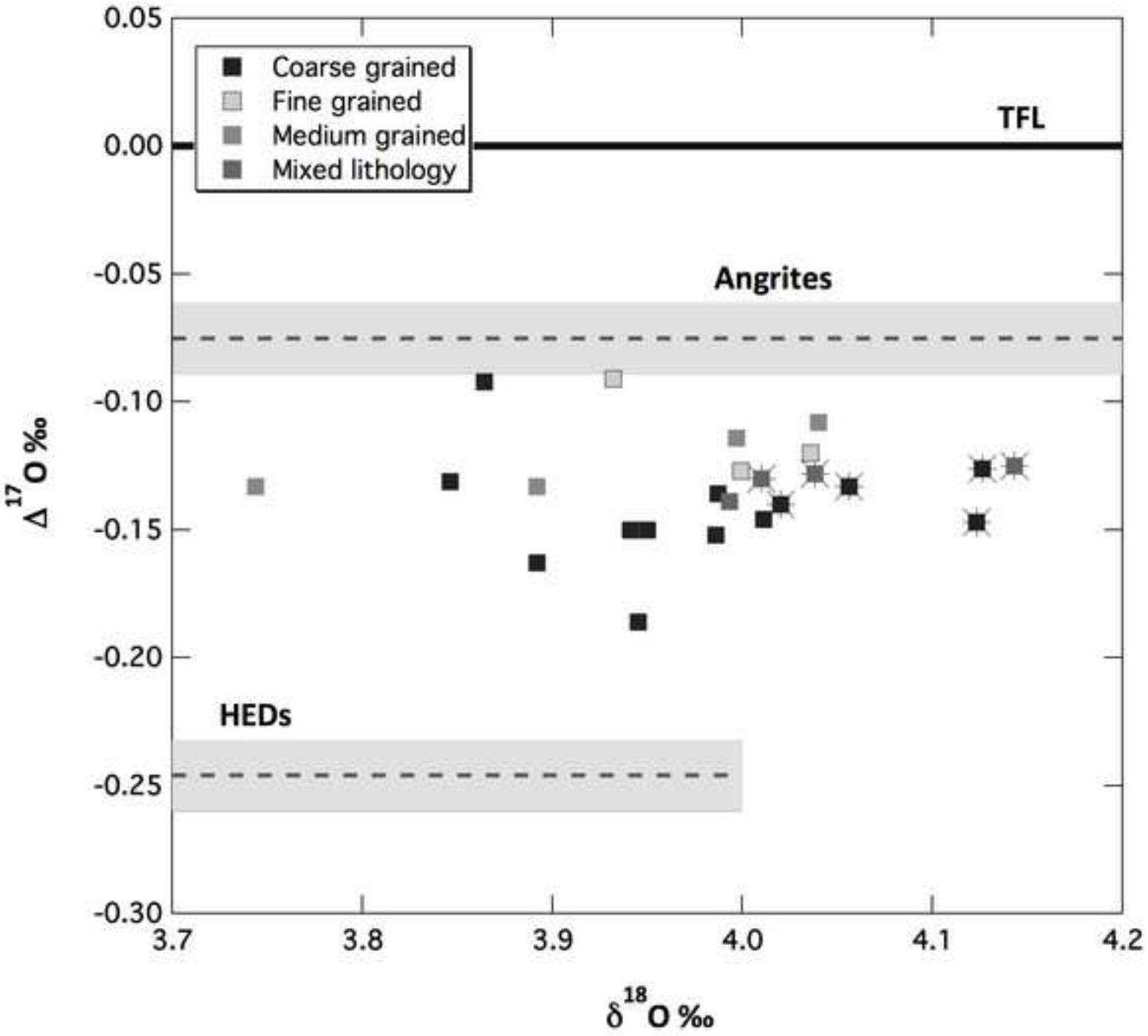

Figure 3

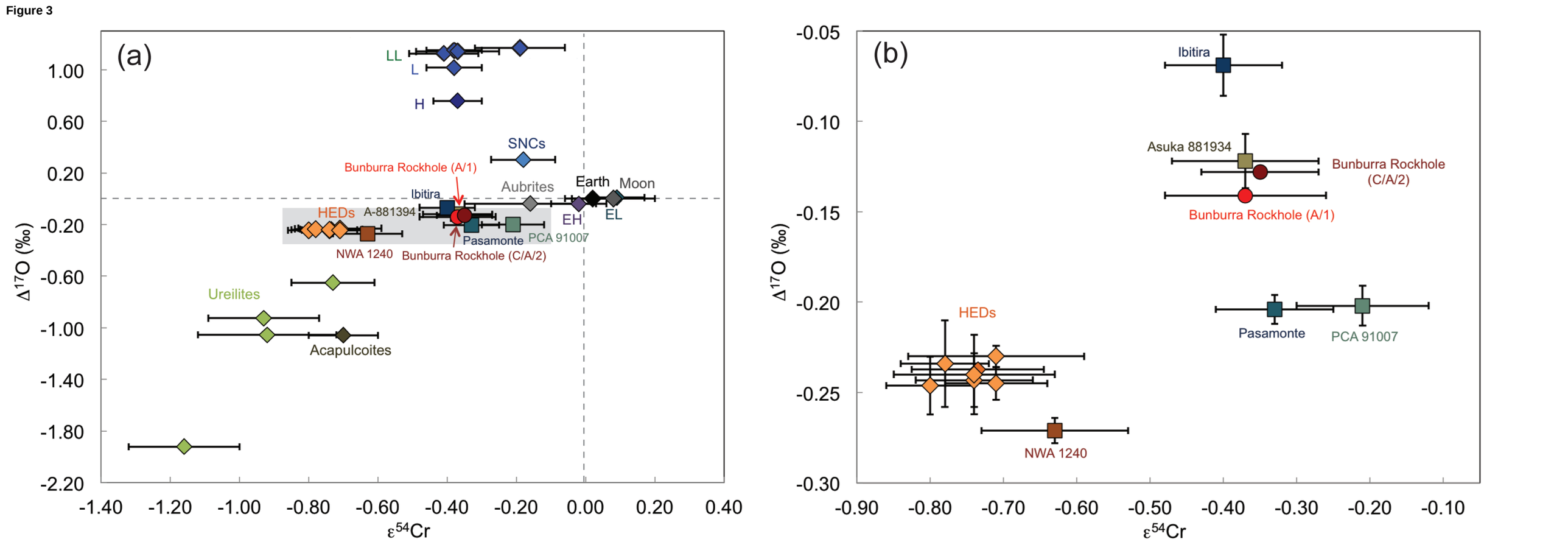
(a)
LL
L
H
SNCs
Bunburra Rockhole (A/1)
Aubrites
Earth
Moon
Ibitira
HEDs
A-881394
EH
EL
Pasamonte
PCA 91007
NWA 1240
Bunburra Rockhole (C/A/2)
Ureilites
Acapulcoites
1.00
0.60
0.20
-0.20
-0.60
-1.00
-1.40
-1.80
-2.20
-1.40
-1.20
-1.00
-0.80
-0.60
-0.40
-0.20
0.00
0.20
0.40
Δ17O (‰)
ε54Cr
(b)
Ibitira
Asuka 881934
Bunburra Rockhole (C/A/2)
Bunburra Rockhole (A/1)
HEDs
Pasamonte
PCA 91007
NWA 1240
-0.05
-0.10
-0.15
-0.20
-0.25
-0.30
-0.90
-0.80
-0.70
-0.60
-0.50
-0.40
-0.30
-0.20
-0.10
Δ17O (‰)
ε54Cr

Figure 4

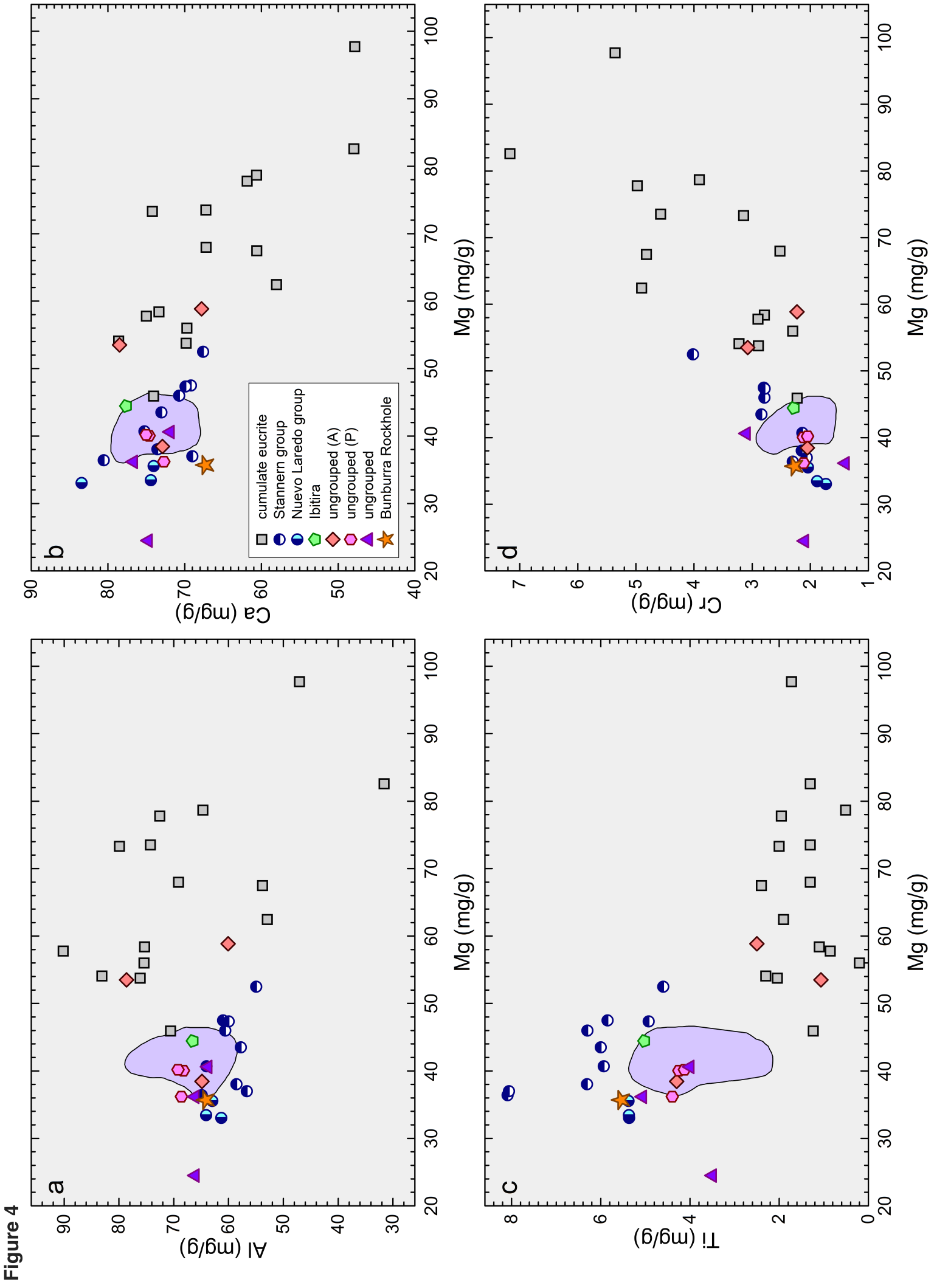

Figure 4

Figure 5

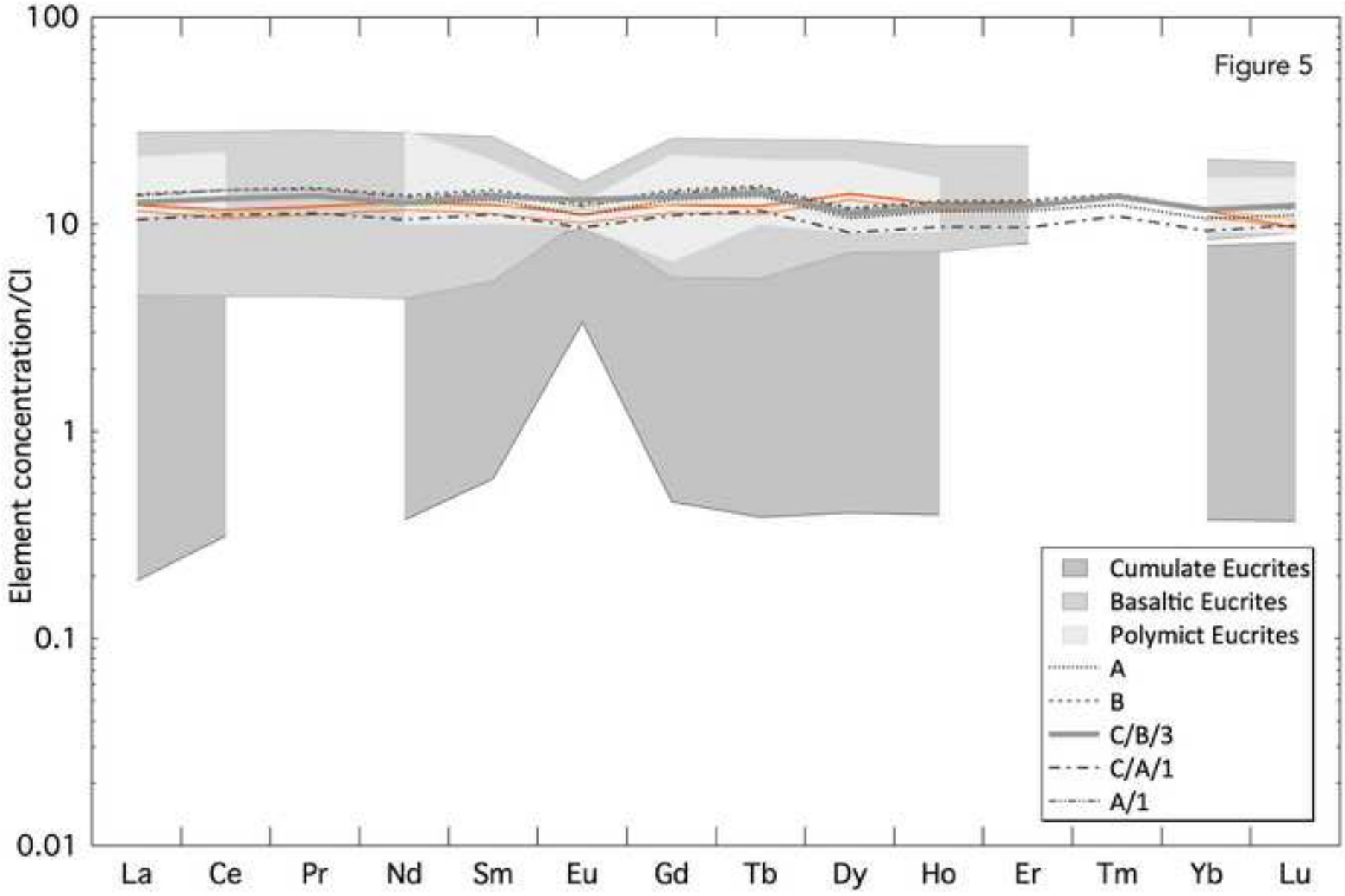

Figure 6

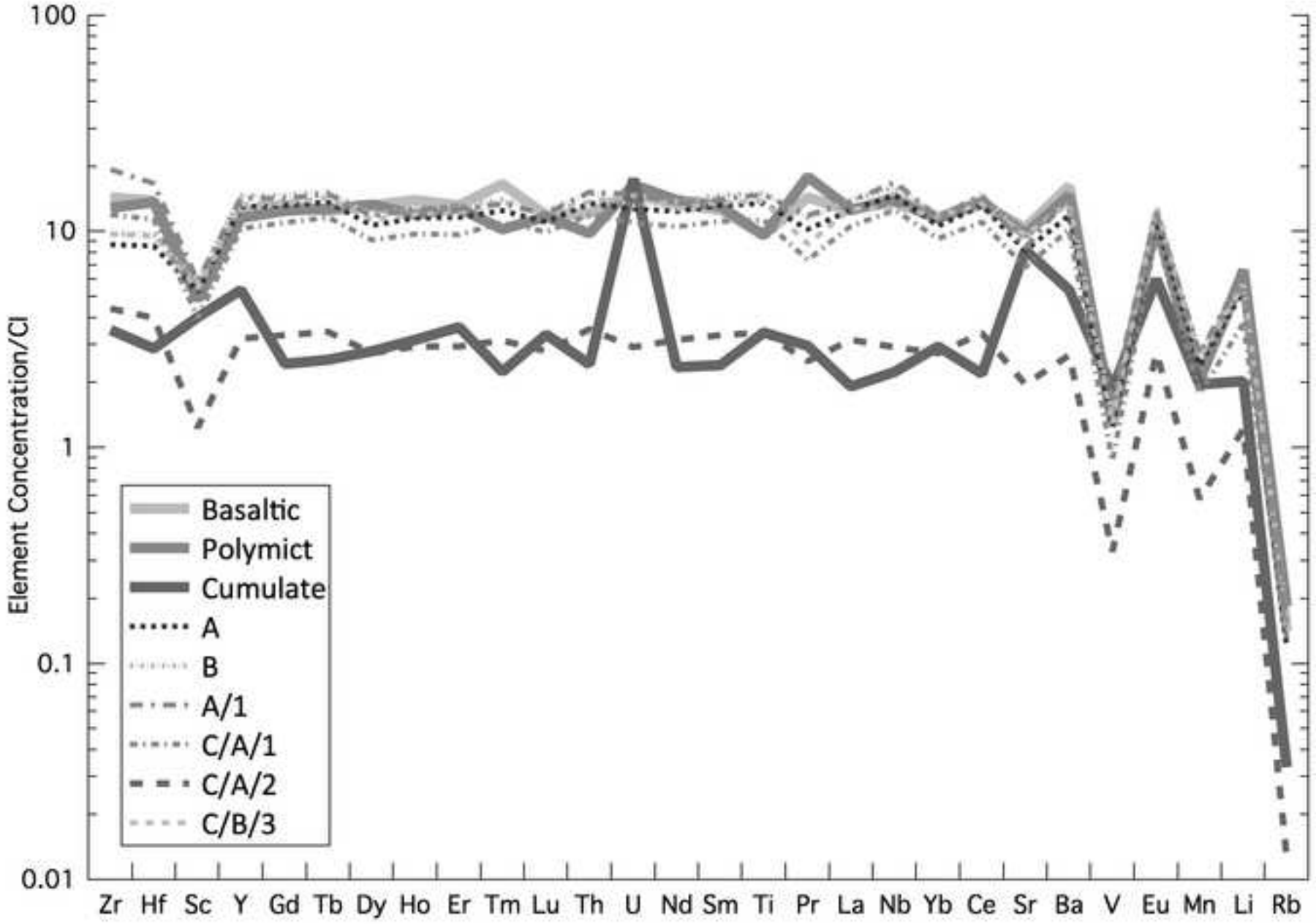

Figure 7

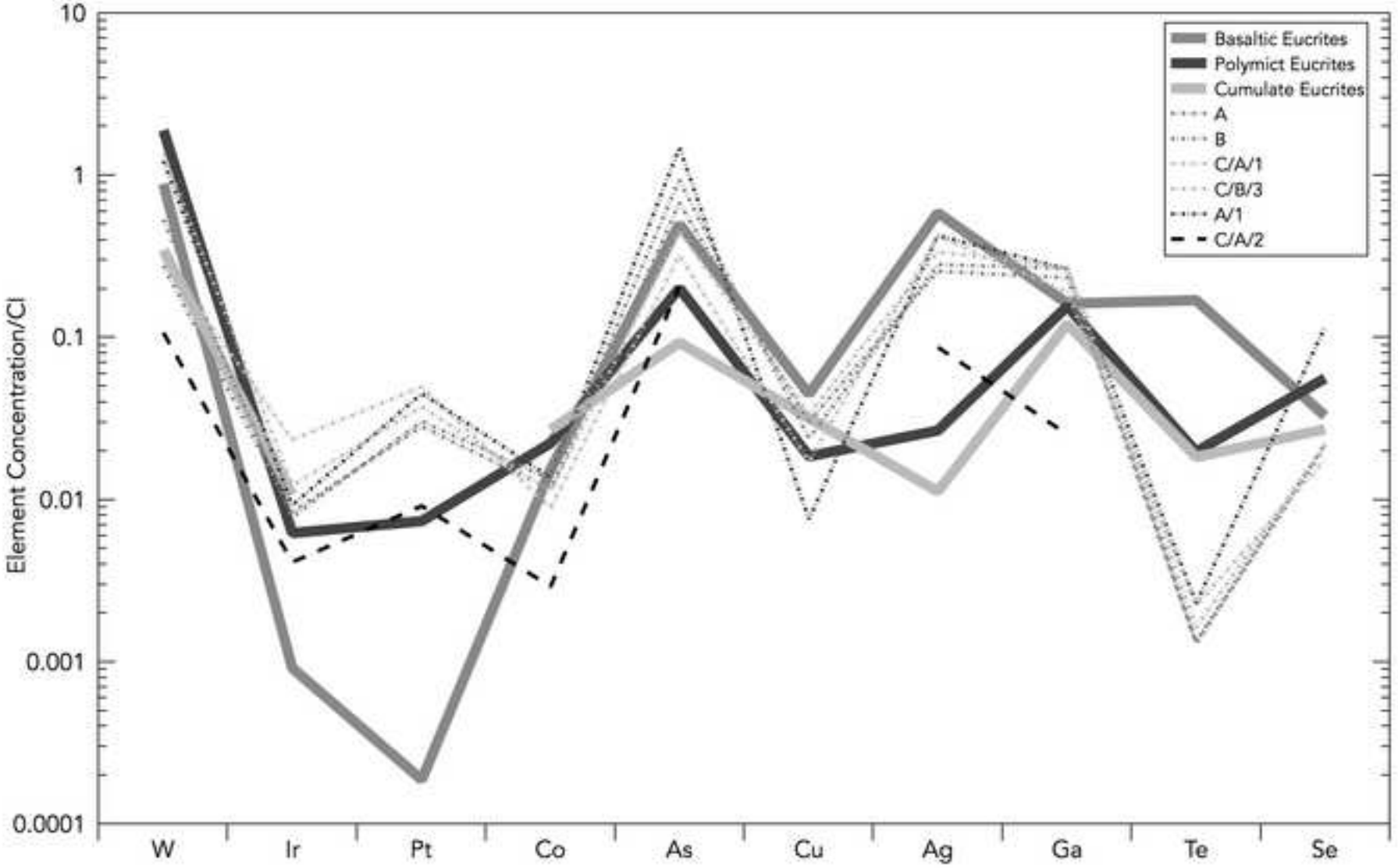

Figure 8

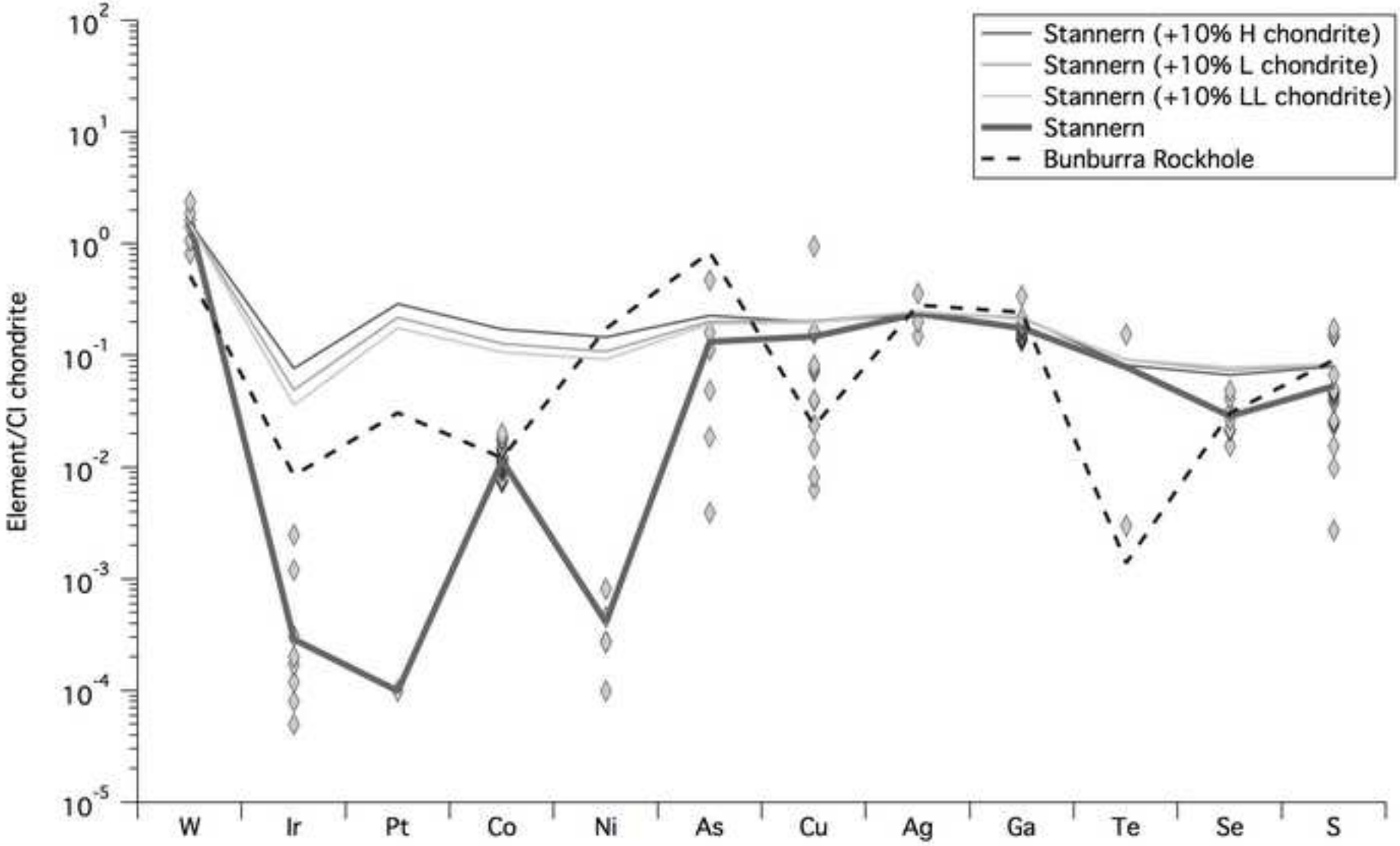

Tables

Table 1. Sample designations, masses, form type analysis type and method of analysis for targeted pieces analysed in this study.

Sample designation	Mass (mg)	Form	Oxygen isotopes	Chromium isotopes	Major elements	Trace elements
A	400	Chip	X		X	X
B	600	Chip			X	X
A/1	112	Powder	X	X		X
C/A/1	30	Powder	X		X	X
C/A/2	50	Powder	X	X		X
C/B/3	40	Powder	X		X	X
SM	400	Powder			X	
Analytical Method			Laser Fluorination	TIMS	ICPMS & XRF *	ICPMS & XRF*

*see table 3

Table 2. Oxygen ($\delta^{17}O$, $\delta^{18}O$ and $\Delta^{17}O$) and Chromium ($\varepsilon^{54}Cr$) isotope compositions for Bunburra Rockhole. Oxygen analyses for Bunburra Rockhole were carried out in three batches (2009, 2012, and 2013). For comparison, average oxygen isotope analyses for HEDs (data from Greenwood et al., 2016) and the obsidian internal standard are included. The sample name includes information about the dominant grain size of the sample; C=coarse grained, M=medium grained, F=fine grained, and Mx =mixed lithology. Bolded values denote the targeted pieces analysed for trace and major element abundances presented in this study.

SAMPLE NAME	N	$\delta^{17}O$	*1σ*	*2σ*	*SEM*	*2*SEM*	$\delta^{18}O$	*1σ*	*2σ*	*SEM*	*2*SEM*	$\Delta^{17}O‰_{linea}$	*1σ*	*2σ*	*SEM*	*2*SEM*	$\varepsilon^{54}Cr$	*Error*
BR-F1	5	1.970	*0.039*	*0.077*	*0.017*	*0.035*	3.932	*0.058*	*0.117*	*0.026*	*0.052*	-0.091	*0.014*	*0.028*	*0.006*	*0.013*		
BR-M1	3	1.981	*0.014*	*0.027*	*0.008*	*0.016*	3.997	*0.023*	*0.046*	*0.013*	*0.027*	-0.114	*0.002*	*0.005*	*0.001*	*0.003*		
BR-M2	2	1.829	*0.054*	*0.107*	*0.038*	*0.076*	3.744	*0.110*	*0.219*	*0.078*	*0.155*	-0.133	*0.004*	*0.007*	*0.003*	*0.005*		
BR-C1	3	1.885	*0.022*	*0.044*	*0.013*	*0.025*	3.846	*0.060*	*0.120*	*0.035*	*0.070*	-0.131	*0.012*	*0.024*	*0.007*	*0.014*		
BR-C2	2	1.933	*0.065*	*0.130*	*0.046*	*0.092*	3.864	*0.124*	*0.249*	*0.088*	*0.176*	-0.092	*0.000*	*0.000*	*0.000*	*0.000*		
BR-F2	2	1.995	*0.003*	*0.006*	*0.002*	*0.004*	4.036	*0.008*	*0.017*	*0.006*	*0.012*	-0.120	*0.002*	*0.003*	*0.001*	*0.002*		
BR-M3	1	1.907					3.892					-0.133						
BR-C/F	1	1.937					3.986					-0.152						
BR-C3	1	1.882					3.945					-0.186						
Mixed-Mx1	2	1.954	*0.109*	*0.218*	*0.077*	*0.154*	3.993	*0.216*	*0.431*	*0.153*	*0.305*	-0.139	*0.004*	*0.008*	*0.003*	*0.006*		
Medium grained-M4	1	2.010					4.040					-0.108						
Coarse grained-C5	2	1.956	*0.031*	*0.062*	*0.022*	*0.044*	4.011	*0.070*	*0.140*	*0.049*	*0.099*	-0.146	*0.006*	*0.011*	*0.004*	*0.008*		
A-C6	**1**	**2.080**					**4.233**					**-0.139**						
A-C7	**1**	**1.993**					**4.056**					**-0.133**						
A-C8	**1**	**2.037**					**4.126**					**-0.126**						
A-C9	**1**	**2.014**					**4.123**					**-0.147**						
A/1-C10	**2**	**1.967**	***0.016***	***0.033***	***0.012***	***0.023***	**4.020**	***0.027***	***0.054***	***0.019***	***0.038***	**-0.140**	***0.002***	***0.004***	***0.002***	***0.003***	**-0.37**	***0.11***
C/A/1-Mx2	**2**	**2.047**	***0.021***	***0.041***	***0.015***	***0.029***	**4.143**	***0.039***	***0.078***	***0.027***	***0.055***	**-0.125**	***0.000***	***0.000***	***0.000***	***0.000***		
C/A/2-Mx	**2**	**1.988**	***0.010***	***0.020***	***0.007***	***0.014***	**4.038**	***0.011***	***0.021***	***0.007***	***0.015***	**-0.128**	***0.004***	***0.009***	***0.003***	***0.006***	**-0.35**	***0.08***
C/B/3-Mx3	**2**	**1.972**	***0.035***	***0.071***	***0.025***	***0.050***	**4.010**	***0.055***	***0.110***	***0.039***	***0.078***	**-0.130**	***0.006***	***0.013***	***0.005***	***0.009***		
Area A - C11	1	1.954					3.987					-0.136						
Area A - F3	1	1.969					3.999					-0.127						
Area A - C12	1	1.920					3.950					-0.150						
Area A - C13	1	1.877					3.892					-0.163						
Area A - C14	1	1.916					3.941					-0.150						
AVERAGE	42	1.959	*0.058*	*0.116*	*0.009*	*0.018*	3.992	*0.104*	*0.207*	*0.016*	*0.032*	-0.134	*0.020*	*0.041*	*0.003*	*0.006*		
Average	**12**	**2.012**	***0.040***	***0.079***	***0.006***	***0.012***	**4.094**	***0.076***	***0.153***	***0.012***	***0.024***	**-0.133**	***0.008***	***0.016***	***0.001***	***0.002***	**-0.36**	***0.10***
HEDS (FALLS ONLY)*	26	1.642	*0.112*	*0.224*	*0.022*	*0.044*	3.591	*0.219*	*0.437*	*0.043*	*0.086*	-0.240	*0.007*	*0.014*	*0.001*	*0.003*		
Obsidian internal standard	39	3.808	*0.026*	*0.052*	*0.004*	*0.008*	7.267	*0.047*	*0.094*	*0.008*	*0.015*	0.001	*0.009*	*0.018*	*0.001*	*0.003*		

Note: 1σ and 2σ represent one and two times the ***standard deviation*** of the replicate analyses, while SEM is the ***standard error of the mean*** (=σ/sqrt(N)); see results section for more details.

Table 3. Bulk major and minor elements in Bunburra Rockhole (reported in mg/g). Pieces A, B, C/A/1 and C/B/3 were analyzed using ICP-MS, while piece SM was 0.4g of powder, homogenized from a 1g piece, analyzed by X-ray Fluorescence. Also included is the weighted average of all pieces by all methods (by sample mass – see table 1) along with the standard deviation (2σ)

Method	*ICP-MS*	*ICP-MS*	*ICP-MS*	*ICP-MS*	*XRF*		
Element	A	B	C/A/1	C/B/3	SM	Weighted Avg	σ
Si	*265**	*251**		*215.56**	209.82	231.65	*62.65*
Ti	4.50	5.09	3.26	3.87	7.07	5.39	*1.22*
Al	57.12	60.22	49.23	71.59	74.58	63.37	*8.28*
Cr	2.13	2.34	1.77	2.77	2.30	2.27	*0.16*
Fe	126.20	135.87	107.82	157.88	150.23	137.17	*11.68*
Mn	3.87	4.17	3.37	4.82	5.73	4.51	*0.86*
Mg	32.07	34.83	26.52	40.34	39.74	35.40	*3.63*
Ca	64.45	68.12	56.11	77.88	68.18	67.16	*3.22*
Na	2.46	2.54	1.96	3.18	4.60^	2.46	*1.26*
K	0.27	0.28	0.26	0.29	1.33^	0.38	*0.56*
P	0.25	0.22	0.18	0.23	0.27	0.24	*0.03*
S					0.57	0.16	*0.28*
Ni					1.91	0.52	*0.95*

*Si values were not measured; they were calculated as the difference between the measured cations and an assumed total of 100 wt% (see methodology).
^Na and K are anomalously high in the XRF data (piece SM). A different weighting is applied to these in determining the weighted average. See discussion in results section.

Table 4. Bulk trace elemental abundances in Bunburra Rockhole as determined by ICP-MS. Rare earth elements are italicized.

Mass		400 mg	600 mg	40 mg	30 mg	112 mg	50 mg
Element	unit	A	B	C/B/3	C/A/1	A/1*	C/A/2*
Li	µg/g	8.0	8.6	8.6	5.6	9.6	1.8
Sc	µg/g	30.6	34.4	31.6	23.3	34.2	7.2
V	µg/g	70.6	81.2	73.7	49.0	95.5	18.6
Co	µg/g	5.8	6.7	5.6	4.4	6.9	1.5
Cu	µg/g	3.8	3.0	4.3	2.2	1.0	bdl
Ga	µg/g	2.3	2.7	2.7	1.9	2.6	0.3
As	µg/g	1.3	1.7	0.8	0.6	2.8	0.4
Se	ng/g	396	410	406	327	2174	620
Rb	ng/g	276	328	381	302	360	29
Sr	µg/g	63.8	73.8	74.9	53.4	65.7	15.3
Y	µg/g	20.3	22.9	20.8	16.1	22.4	5.0
Zr	µg/g	34.3	38.6	38.4	47.2	76.5	17.4
Nb	µg/g	3.6	4.0	3.2	3.1	4.2	0.7
Ag	ng/g	51	56	67	84	85	17
Te	ng/g	3	3	4	5	5	bdl
Ba	µg/g	27.8	31.9	31.9	24.1	34.2	6.3
La	*µg/g*	2.9	3.3	3.0	2.5	3.2	0.7
Ce	*µg/g*	8.0	8.9	8.1	6.7	8.9	2.0
Pr	*µg/g*	1.2	1.3	1.2	1.0	1.3	0.3
Nd	*µg/g*	5.6	6.3	5.8	4.8	6.1	1.4
Sm	*µg/g*	1.9	2.2	2.0	1.6	2.1	0.5
Eu	*ng/g*	623	706	737	544	685	153
Gd	*µg/g*	2.6	2.9	2.7	2.2	2.8	0.7
Tb	*ng/g*	497	556	518	423	542	125
Dy	*µg/g*	2601	2915	2739	2216	2865	664
Ho	*ng/g*	644	723	671	542	708	163
Er	*µg/g*	1.8	2.1	1.9	1.5	2.0	0.5
Tm	*ng/g*	302	339	332	267	325	76
Yb	*µg/g*	1.7	1.9	1.9	1.5	1.9	0.4
Lu	*ng/g*	270	303	300	242	293	68
Hf	ng/g	896	1008	993	1183	1741	415
W	ng/g	26	49	126	28	114	10
Ir	ng/g	8	8	12	24	9	4
Pt	ng/g	14	15	18	24	22	4
Th	ng/g	397	442	404	351	448	104
U	ng/g	103	107	119	89	121	24

bdl = delow detection limit.
*Pieces analyzed for Cr isotopes.